The San Francisco Bay Area —

On *Shaky* Ground

April 1995

ASSOCIATION OF BAY AREA GOVERNMENTS

The San Francisco Bay Area --

On *Shaky* Ground

APRIL 1995

ASSOCIATION OF BAY AREA GOVERNMENTS
Mailing Address: P.O. Box 2050 -- Oakland, CA 94604-2050
Location: Joseph P. Bort MetroCenter -- Eighth and Oak Streets -- Oakland
Phone: (510) 464-7900 -- Fax: (510) 464-7970
Internet Access through abagOnline at http://www.abag.ca.gov

Publication Number: P95001EQK

CREDITS ...

Report Authors:

Jeanne B. Perkins -- Earthquake Program Manager, Assoc. of Bay Area Governments
John Boatwright -- Geophysicist, U.S. Geological Survey

Technical Support:

Paul Wilson -- President, MapFrame Corp. -- GIS software and support
Bryan Magers and Michael Dufner, ABAG -- Internet publication assistance

ABAG Management:

Eugene Y. Leong -- Executive Director
Gary Binger -- Planning Director

Acknowledgments:

ABAG would like to acknowledge the efforts of several reviewers, including David M. Boore and Carl Mortensen who handled the internal review of the U.S. Geological Survey, and the following members of two ABAG Review Committees:

ABAG Earthquake Mapping for Local Governments Review Committee:

Catherine Bauman -- Planning Dept., City and County of San Francisco
Ed Bortugno -- Geologist, California Office of Emergency Services
Dan Berman -- GIS Manager, City of San Ramon
Leslie Carmichael -- Senior Planner, City of Foster City
John Lane -- Building Rehabilitation Supervisor, Office of Emerg. Services, City of San Jose
Dale Marcum -- Geologist/Geotechnical Engineer, City of Saratoga (Wm. Cotton and Assoc.)
Carl Mortensen -- Geophysicist, U.S. Geological Survey
Carol Prentice -- Geologist, U.S. Geological Survey
Richard Scott -- Prin. Engineering Technician, City of Novato
Grant Wilson -- Planning Consultant, City of San Bruno

ABAG Earthquakes and Housing Losses Review Committee:

Thelma Rubin -- Committee Chair -- Mayor, City of Albany
Christopher Arnold -- President, Building Systems Development (BSD), Inc.
Roger Borcherdt -- Geophysicist, U.S. Geological Survey
John Harrald -- Assoc. Professor, Engineering Management, George Washington University
Laurence Kornfield -- Chief Building Inspector, City and County of San Francisco
Frank McClure -- Consulting Structural Engineer
Patrick McClellan -- Earthquake Preparedness Coordinator, City of San Leandro Fire Dept.
Gregg O'Ryon -- Director, Disaster Services, American Red Cross - Bay Area
Paula Schulz -- State Hazard Mitigation Officer, California Office of Emergency Services
Roy Schweyer -- Mgr., Housing & Neigh. Preservation, Off. of Comm. Dev., Oakland
Martha Blair Tyler -- Spangle Associates, Urban Planning and Research
Frannie Winslow -- Director, Office of Emergency Services, City of San Jose

PHOTO CREDITS - Page 11 - Dave Rogers; Page 12 - Degenkolb Assoc.; Page 14 (top) and 19 - Jeanne Perkins, Page iv and 14 (bottom) - Anonymous
CARTOGRAPHY - Eureka Cartography (Berkeley, CA) using ABAG's geographic information system (BASIS) maps
COVER GRAPHICS - Peter Beeler using ABAG's geographic information system (BASIS) map of geologic materials

The writing and production of this report was financed in part with Grant No. 1434-94-G-2394 from the U.S. Geological Survey (USGS). Additional funds have been provided by ABAG. The research is based upon work by the authors supported by National Science Foundation (NSF) Grant No. BCS-9302612 and USGS Project No. 9930-12343. Any opinions, findings, conclusions or recommendations expressed in this material are those of the authors and do not necessarily reflect the views of NSF or USGS.

TABLE OF CONTENTS ...

BACKGROUND ...

During the last twenty years, ABAG, with funding from both the U.S. Geological Survey and the National Science Foundation, has developed a number of earthquake hazard maps for the nine-county San Francisco Bay Area. Those maps were last revised in the mid-1980s and resulted in the publication in 1987 of the first ***On Shaky Ground*** report. The Loma Prieta earthquake in 1989 and the Northridge earthquake in 1994 were devastating in their effects on northern and southern California. However, they have also provided us with valuable information to test the hypotheses forming a basis for those earlier maps and to develop a better understanding of the physical processes that occur in earthquakes. The maps described and shown on the following pages are the result of this research and better understanding. They are an updated version of the maps documented in the 1987 ***On Shaky Ground*** report.

This report documents ABAG's shaking hazard maps to encourage appropriate planning for and mitigation of earthquake hazards.

THE IMPORTANCE OF SHAKING HAZARD MAPS ...

Maps included in this report are for the entire San Francisco Bay Area. Maps for individual cities are available from ABAG's offices and on the Internet at abagOnline at http://www.abag.ca.gov. City maps are detailed enough to show street patterns. *(See page 10.)*

The San Francisco Bay Area is in "earthquake country."

In ***some*** earthquakes, the surface of the ground can rupture along a fault -- or a landslide can be triggered -- or underground sand layers may flow (liquefy) -- or a tsunami ("tidal" wave) may be generated in water. ***But in ALL earthquakes, the ground shakes.*** In large magnitude earthquakes, more ground shakes, and it shakes longer, than in small magnitude earthquakes. Ground shaking causes damage tens of miles away from the fault source.

When the ground shakes, damage occurs to buildings, facilities and their contents. People can be injured or killed. People find that they may no longer be able to sleep in their homes, or even have access to their belongings. Businesses can't function and segments of the economy suffer. Hazardous materials are released which can be damaging to people and the environment.

Various options are available to avoid, reduce or otherwise mitigate these results. What YOU do to prepare for shaking can minimize or eliminate these effects.

Most earthquake damage is caused by the shaking of the ground itself. Yet, at the same time, many existing local and State government hazard reduction programs and regulations focus on other earthquake hazards. Our purposes in preparing this booklet are to expose ground shaking as a significant hazard, to show (using maps) the areas with the strongest expected shaking, and to suggest ways to mitigate shaking damage.

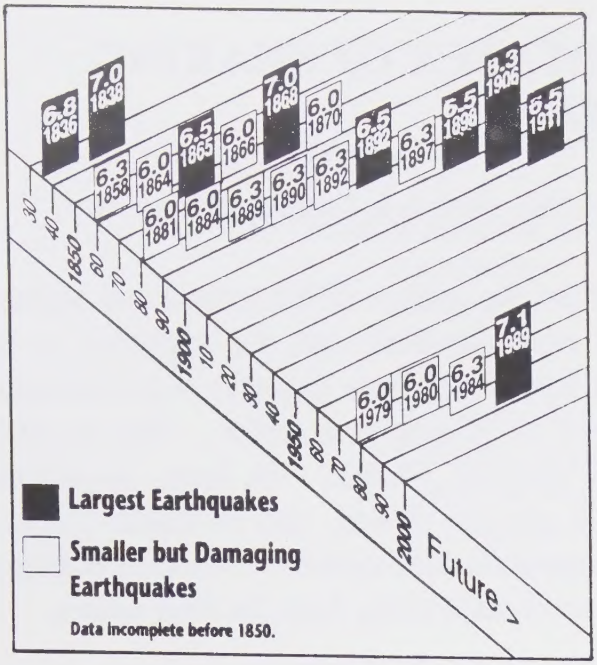

Estimated magnitude and year of occurrence are shown. Note that the level of earthquake activity in the last 15 years is closer to the period prior to the 1906 San Francisco earthquake, while the 1911 to 1979 period, when most of the Bay Area developed, is exceptionally quiet. Courtesy of Peter Ward, USGS.

THE BAY AREA IS EARTHQUAKE COUNTRY...

The fact that a devastating earthquake occurred in 1906 -- the San Francisco earthquake -- is common knowledge. Larger earthquakes generally affect larger areas; the ***San Francisco*** earthquake caused extensive damage in Oakland, San Jose and Santa Rosa. More recently, the 1989 Loma Prieta earthquake caused extensive damage in the Santa Cruz Mountains, as well as in Oakland and San Francisco tens of miles away. But many moderate to great earthquakes (over magnitude 6.0) have affected the Bay Area; 22 such events have occurred in the last 160 years -- for an average of one every seven years.

Earthquakes occur in the Bay Area when forces underground cause the faults beneath us to rupture and suddenly slip. If the rupture extends to the surface, we see movement on a fault (surface rupture). But strong earthquakes can occur when the fault rupture does not extend to the surface. The fault rupture of the ground generates vibrations or waves in the rock which we feel as ground shaking. Because faults are weaknesses in the rock, earthquakes tend to occur over and over on these same faults. Almost all of the major faults in the Bay Area are ***strike-slip faults*** where the rupture extends almost vertically into the ground and the ground on one side moves ***past*** the ground on the other side of the fault. ***Thrust faults***, where ground moves ***over*** adjacent ground, are much more common in the Los Angeles area than the Bay Area because the San Andreas fault makes a large bend to the west there before heading northwest. Thrust faults in southern California are caused by this bending.

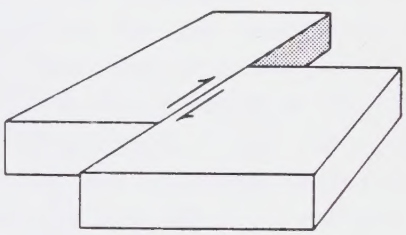

Strike-Slip Fault Diagram

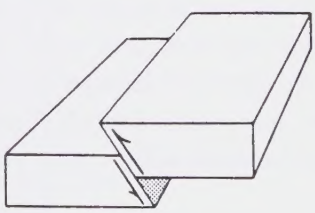

Thrust Fault Diagram

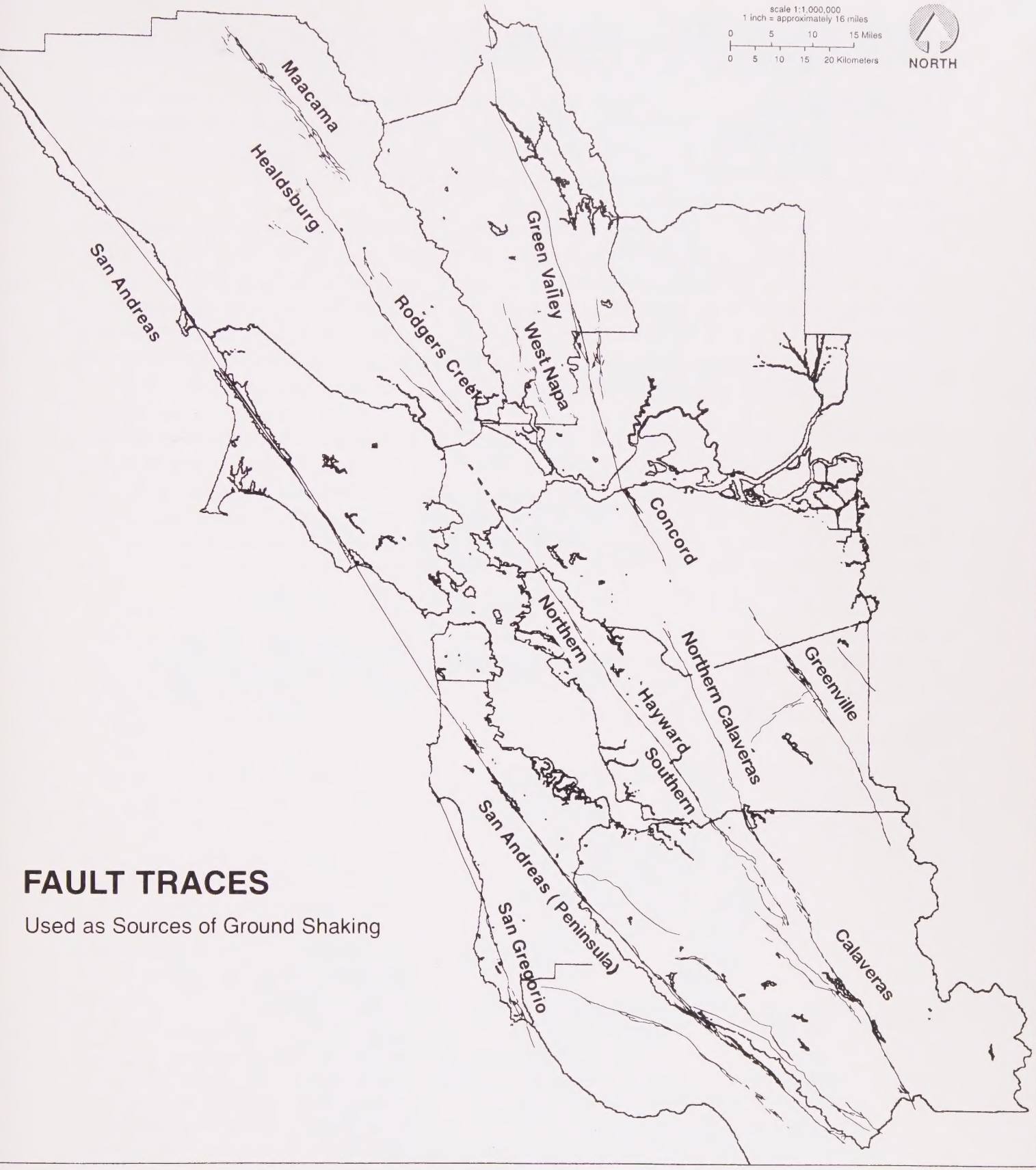

FAULT TRACES

Used as Sources of Ground Shaking

Source: *On Shaky Ground* – 1995

ABAG©

Association of Bay Area Governments

HOW BIG IS BIG -- MEASURING EARTHQUAKE SIZE

Magnitude is a measure of overall earthquake size.

Larger magnitude earthquakes generally cause a larger area of ground to shake hard, and to shake longer. This relationship is generally well understood. Thus, one principal factor in determining shaking hazard is the magnitude of the earthquake.

Seismologists now have several measures of earthquake magnitude in addition to the familiar Richter (or "local") magnitude. The Richter magnitude has difficulty differentiating the size of large and great (7-1/2+) magnitude earthquakes. To overcome this difficulty, modern seismologists use ***moment magnitude*** because it best reflects the energy released by the earthquake. The moment magnitude is proportional to the area of the fault surface that has slipped. Thus, it is directly related to the fault length. Because the models used to generate the shaking hazard maps in this report are based on fault length, they, in effect, bypass magnitude. (See Appendix A.)

Fault segments generate ***"characteristic"*** earthquakes. Some faults are weak and tend to generate earthquakes with moment magnitudes of 5 and 6. However, at least ten fault segments in the Bay Area are relatively strong and can store up enough energy to generate earthquakes of magnitude 7 or so. These stronger faults will generate these large earthquakes, not magnitude 5 and 6 events. The concept of "characteristic" earthquakes means that we can anticipate, with reasonable certainty, the actual damaging earthquakes that will occur on these fault segments. These anticipated events are the ***scenario earthquakes*** depicted in the color maps in the center section of this report.

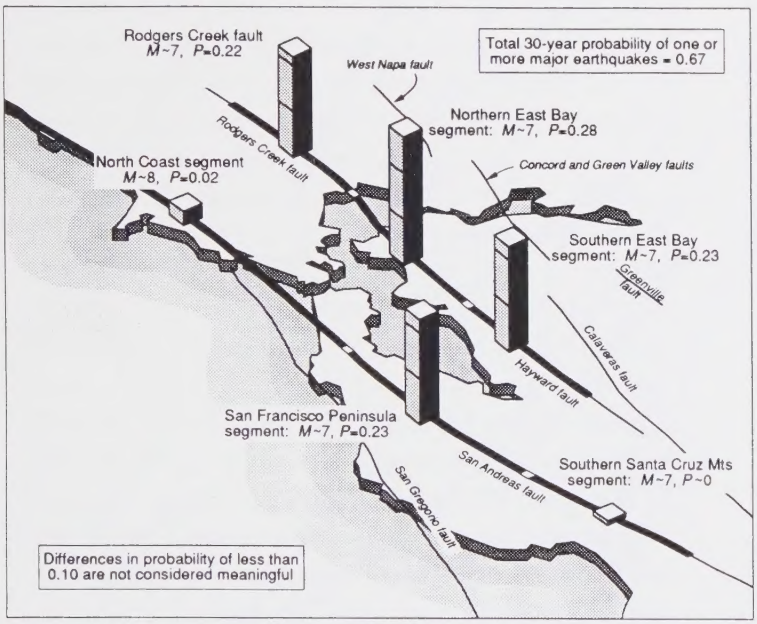

30-YEAR PROBABILITIES (*P*) OF LARGE EARTHQUAKES (*M*≥7) IN THE SAN FRANCISCO BAY REGION

Column heights are proportional to 30-year probability of earthquake rupture

Courtesy of the U.S. Geological Survey (Ref. 3)

The probability of one of these scenario earthquakes occurring varies from fault segment to fault segment. The two Hayward fault segments and the peninsula segment of the San Andreas are felt to have, roughly, a probability of one in four of occurring in the next 30 years (Ref. 3). Other fault segments are less well understood; equivalent probabilities are being developed.

Note: No probability data is provided in Ref. 3 for the entire Hayward fault rupturing at once. However, experts at the U.S. Geological Survey working on a map to be included in the Uniform Building Code are now assuming that one in every four Hayward earthquakes will involve both segments of the Hayward rupturing at once, yielding a probability of 5-6% in 30 years (personal communication, Art Frankel).

HOW STRONG IS STRONG -- MEASURING SHAKING

Intensity is a measure of the effect of the earthquake at a specific location.

Just as a light bulb above my desk is 100 watts regardless of where I'm sitting, and the intensity of the light varies with where I am in my office, an earthquake has a single moment magnitude and a variety of intensities distributed throughout the region.

Jeanne Perkins

An earthquake has one moment magnitude, but a range of intensities. The most commonly used intensity scale is the modified Mercalli intensity scale (MMI scale). The intensity of ground shaking at a site varies for any particular earthquake based on several factors:

- the size (magnitude) of the earthquake (which is related to the length of the fault that ruptures);
- the distance from the site to the fault source for the earthquake;
- the directivity (focusing of earthquake energy along the fault axis rather than perpendicular to the fault); and
- the type of geologic material underlying the site, with stronger shaking occurring on softer soils.

The map of predicted intensities for the 1989 Loma Prieta earthquake is shown on page 21 to provide a general sense of intensity. Loma Prieta had a moment magnitude of 6.9.

The following table shows the 11 scenario earthquakes on 10 fault segments in the Bay Area for which intensity maps have been generated. (Both segments of the Hayward fault rupturing at once provides the eleventh scenario.) Approximate magnitudes calculated for the scenario earthquakes can aid in relating these scenarios to past earthquakes. ***As shown by the color maps in the center of this booklet, all of these earthquakes result in areas of modified Mercalli intensities of V to X.***

Moment Magnitude Based on Fault Length for Scenario Earthquakes

Source Fault	Fault Length (in km) (See Note)	Moment Magnitude of Characteristic Earthquake
Hayward	85.0	7.3
San Gregorio	57.1	7.1
Healdsburg-Rodgers Creek	56.5	7.1
Greenville	53.9	7.1
Concord-Green Valley	53.2	7.1
Peninsula Segment of the San Andreas	52.4	7.1
Northern Hayward	49.3	7.1
Southern Hayward	44.7	7.0
Northern Calaveras	37.2	6.9
Maacama	32.3	6.8
West Napa	24.1	6.7

Note : The formula used to estimate moment magnitude for each of these fault segments (from Ref. 48) is:

Moment Magnitude = 5.16 + [1.12 x log (surface fault length in km)]

HOW DISTANCE AND DIRECTIVITY AFFECT SHAKING INTENSITY...

The epicenter is the point on the surface above the location where the fault begins the slip which generates the earthquake. There is a common myth that most damage will occur near the epicenter of the earthquake, or that the epicenter is synonymous with "ground zero." However, the earthquake epicenter is typically ***not*** the point at which most damage occurs. The fault rupture can be tens of miles long and waves are generated along the entire length of the fault.

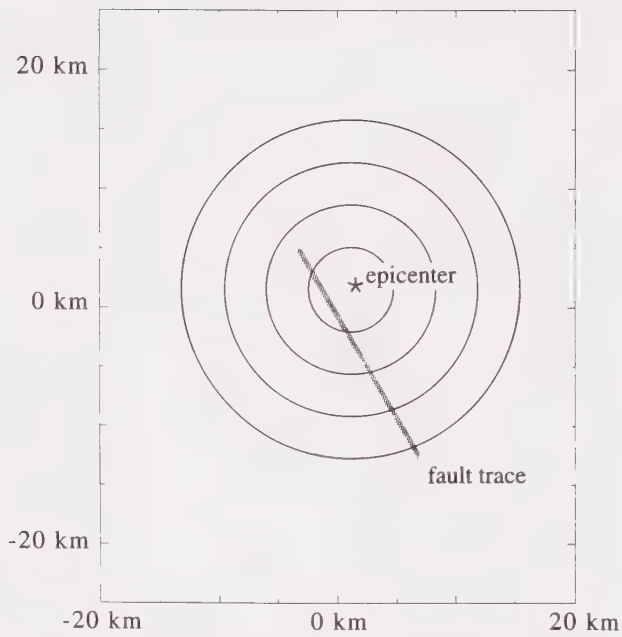

There is a myth of the epicenter. This "donut" pattern is NOT the intensity pattern one should use.

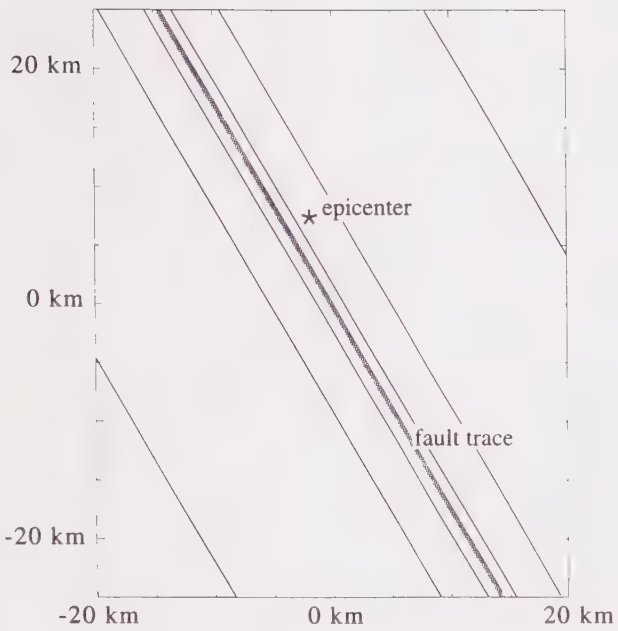

In general, areas closer to the source fault will be shaken more than areas further away.

Thus, predictions of ground shaking intensities are not based on distances from possible epicenters, but on distances from known faults, or segments of faults, on which large earthquakes are anticipated.

Intensity decreases ("attenuates") with distance from the fault. (See Ref. 28.) But the critical distance is not simply the nearest distance to the fault. Seismologists have come to realize that earthquake sources radiate energy at depth; thus, the distance used to attenuate expected shaking must be measured between the site and this underground source. (See Refs. 25, 33, 34, 35, and 38.) However, rupture propagates both upward from this underground source and along the fault axis. (This "directivity" effect is described in the next paragraph.) Thus, there is significant amplification of shaking within a mile of these major fault zones.

Directivity, or focusing of energy along the fault in the direction of rupture, is a significant factor for most large earthquakes in the Bay Area, including the Loma Prieta earthquake. Shaking intensity decreases ("attenuates") much more rapidly perpendicular to the fault rupture plane (or surface fault trace) than along the fault axis. Thus, San Francisco and Oakland, in line with the fault axis, felt stronger shaking than expected in the Loma Prieta earthquake, while San Jose, perpendicular to the fault, felt weaker shaking. The directivity varies with the location of the epicenter. The maps show an "average" directivity since we do not know the location of the epicenter prior to an earthquake. (See Appendix A and Note below.)

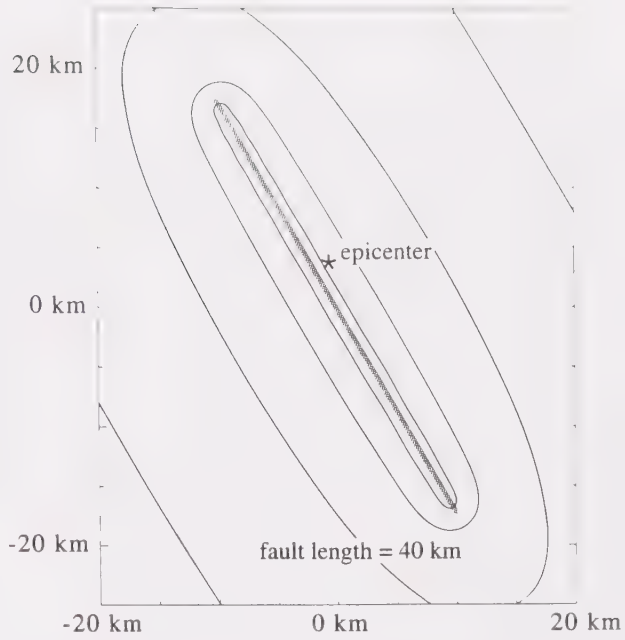

The elongated pattern shows intensity decreasing much more rapidly perpendicular to the fault source than along the fault axis.

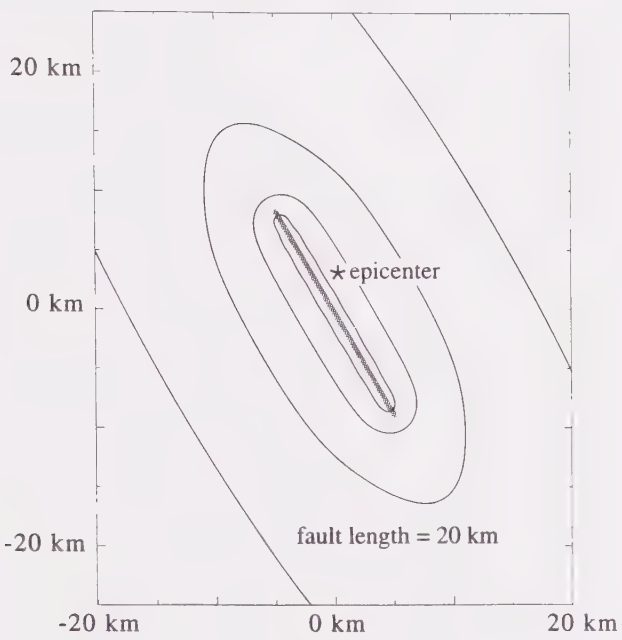

The elongated bands of intensity shrink for earthquakes of smaller moment magnitudes. For the earthquakes of concern to us, modified Mercalli intensities range from V to X, regardless of the moment magnitude of the earthquake.

The final factor affecting the change of intensity with distance from the fault is the magnitude of the earthquake. The intensity boundaries extend further from the fault source for larger magnitude earthquakes. Thus, a site 20 miles from the fault source will experience stronger and longer shaking from an earthquake with a moment magnitude of 7 than from an earthquake with a moment magnitude of 6. Even though the energy released in an earthquake is over thirty times as great in a magnitude 7 quake than a magnitude 6 quake, the shaking is not 30 times as intense. Rather, a larger area is exposed to strong shaking.

Note: One additional factor in the recent Loma Prieta earthquake was the reflection of the seismic waves from the Moho. (The "Moho" is short for the Mohorovicic discontinuity, the boundary between the earth's crust and mantle, and is named for the Croatian scientist who discovered it.) This "bounce" resulted in stronger shaking which ranged from 45 to 60 miles from the fault trace and amounted to somewhere between one-half and one intensity increment level increase over what might have been expected. (See, for example, Ref. 45.) Both Oakland and San Francisco were within this distance band. However, there are insufficient data to reliably calculate such increases for future earthquakes. Because the Loma Prieta earthquake began deeper than is typical for Bay Area earthquakes, this Moho-related increase was probably closer to the fault source than would be expected in future Bay Area earthquakes. Thus, the increase, if it occurs, will be in areas with lower baseline shaking levels and should result in small or insignificant increases in damage.

HOW GEOLOGIC MATERIALS AFFECT SHAKING INTENSITY ...

All ground in the Bay Area was NOT created equal. A critical factor affecting intensity at a site is the geologic material underneath that site. Deep, loose soils tend to amplify and prolong the shaking. The worst such soils in the Bay Area are the loose clays bordering the Bay -- the Bay mud -- and the filled areas. The type of rock that least amplifies the shaking is granite. The remaining materials fall between these two extremes, with the deeper soils in the valleys shaking more than the rocks in the hills. Most development is in the valleys. The map opposite groups the geologic materials in the region into eight categories, each with similar amplification in earthquakes.

If you compare two houses, both of which are the same distance and orientation to the earthquake source, the one on Bay mud will experience stronger and longer shaking than the one on rock.

The role of geologic materials in affecting the intensity of shaking has been known for at least twenty years. Several researchers at the U.S. Geological Survey clearly demonstrated this relationship when they examined data from the 1906 San Francisco earthquake in 1975. (See Ref. 28.) Other researchers have expanded this effort by examining the relationship between intensity and geologic materials. (See Ref. 36.) Although the categories of geologic materials are the same as used in earlier ABAG maps (Refs. 41, 42, 43, and 44), the extent to which these materials modify the shaking intensity has been changed slightly. These susceptibility categories are quite similar, but not identical, to the categories recently developed for use in site-dependent building code provisions. (See Ref. 26.)

The distance-based intensities mapped for each scenario earthquake are increased or decreased based on the shaking amplification potential of each geologic material to produce the final intensity map for each scenario. The extent of these changes ("intensity increments" or fractional changes in intensity units) is listed in Appendix B.

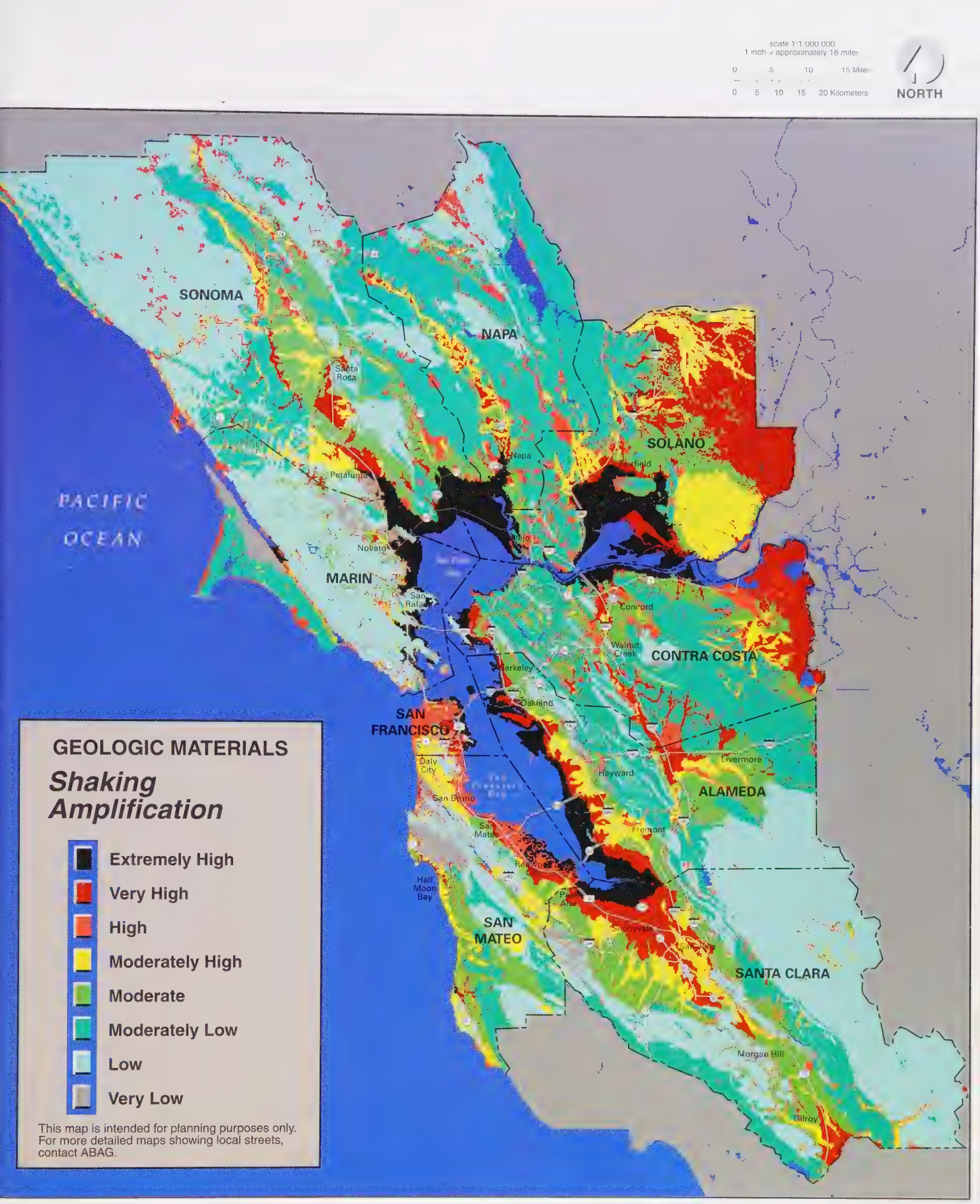

Source: *On Shaky Ground* – 1995

FOR MORE DETAILED INFORMATION ...

These regional maps, as well as maps of smaller (city) areas showing the street network, are available on the Internet on ***abagOnline*** at ***http://www.abag.ca.gov***. Any future modifications or updates of these maps are likely to be available on the Internet prior to "hard copy" publication.

These intensity maps are not intended to be site-specific. Rather, they depict the general risk within neighborhoods, and the relative risk from community to community. Individual intensities can easily be incorrect by plus or minus one intensity unit. See page 20 for a full description of each modified Mercalli intensity category.

Several cities have copies of the critical earthquake scenario intensity maps for their area. You can also examine or obtain copies of maps for individual areas through ABAG. City maps are more detailed and show street patterns, as shown below.

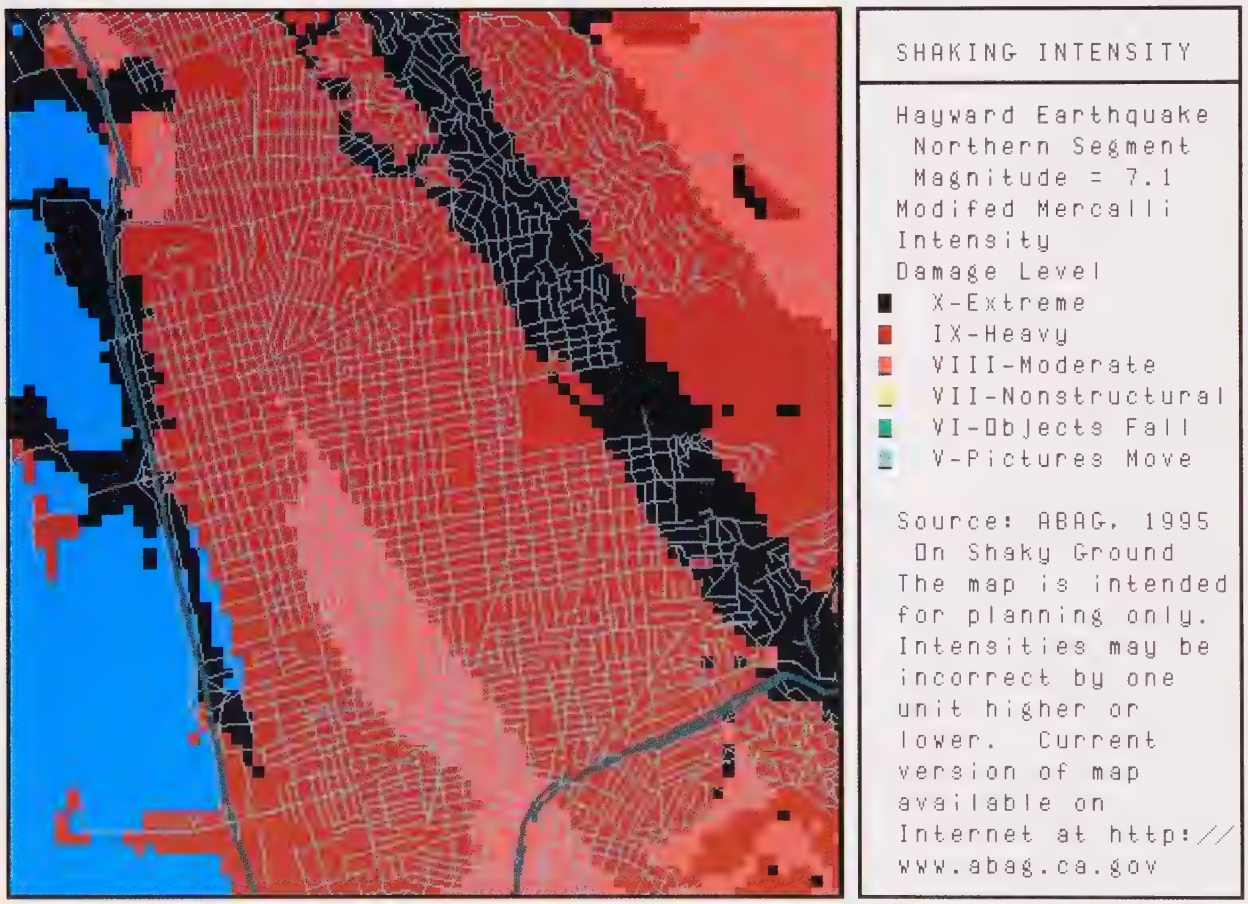

Sample City Map Showing the Cities of Albany and Berkeley

A CALL TO ACTION ...

Better maps can only be truly better if they lead to actions which save lives, reduce suffering and economic hardship, and help protect our environment. What ***you*** do to prepare for shaking can minimize or completely eliminate these effects.

We believe that it is imperative that these revised maps be used for earthquake hazard mitigation and disaster response planning ***now***. ***They depict a significantly larger hazard than the maps previously published.***

Each of the following sections contains general information and recommends additional reports to help you prepare mitigation programs.

ABAG staff are already working to ensure that these maps are used fully by the city and county governments in the Bay Area, by those planning for a better more earthquake-resistant transportation system including the California Department of Transportation (CalTrans), and by relief agencies such as the American Red Cross. But more is needed. It is in this spirit of a call for more ***mitigation*** that the following maps showing the extent of our ***hazard*** are provided to you, the local governments, business owners, homeowners and residents of the San Francisco Bay Area. These maps are also being published on the Internet, at the ***abagOnline*** site at ***http://www.abag.ca.gov***, so that those with access to viewing software such as Mosaic or Netscape on their personal computers can view the regional maps and many local maps.

We all need to take responsibility for making our own homes and workplaces safer so that we can better prepare for the ride of our lives.

WHAT *YOU* CAN DO NEXT ...

As a resident or homeowner:

Most residents must understand that the risk of ***dying*** in an earthquake is extremely low. However, the risk of ***damage*** to your home can be significant, particularly if it is located in a high intensity area.

The most common damage from earthquakes to single-family homes built prior to the 1940s is foundation damage. The "fix" to prevent this damage is to bolt the foundation sill plate to the concrete foundation and to brace or put plywood sheathing on the inside of the "cripple" walls between the foundation and the first floor.

Mobile homes typically fall off the jacks that support them when exposed to intense ground shaking. Again, earthquake bracing systems can be installed to mitigate this problem.

For those who live in apartments or condominiums, the problems are more complex and the solutions more costly. Again, if the buildings were constructed prior to the 1940s, the potential problems are far greater than for newer construction. The spectacular failures to the apartments in the Marina District of San Francisco occurred largely in pre-1940s vintage buildings with parking on the first floor. Parking can even be a problem in buildings built after 1940. For example, many apartments with ground floor parking collapsed or failed in the Northridge earthquake. The tragic deaths at the Northridge Meadows Apartments occurred in a three-story apartment building in which a large portion of the ground floor was parking. When this ground floor parking collapsed, the adjacent ground floor apartments collapsed as well.

Falling objects within your home will likely result in the greatest losses and pose a significant threat of injury. Just because you cannot push something over easily does not mean that the heavy object will not topple, causing injuries.

- Cupboard doors (including sliding doors) can open in earthquakes. Cupboards containing cleaning solutions or other chemicals, or dishes that are valuable, should be fitted with positive latches.
- Heavy bookcases and tall furniture should be screwed to wall studs.
- Your gas hot-water heater should be secured to the wall studs. All gas appliances should be connected to the gas supply with a short piece of flexible tubing. Propane gas storage tanks should be designed not to overturn and roll.
- Mirrors, bookcases and other heavy objects should be anchored or removed from near your beds.

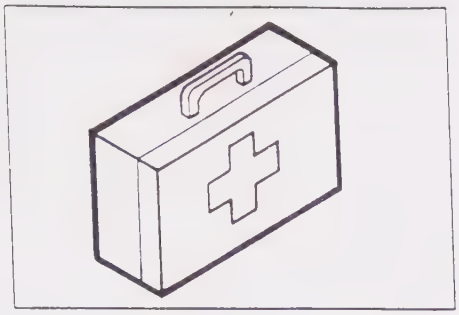

Everyone should have emergency water, food, and prescription medications on hand. First aid and CPR training is also useful.

Recommendations for an "Earthquake Kit" are available from your local Red Cross chapter, local or County Office of Emergency Services, or by looking in the front of your telephone book.

For More Information:

From the American Red Cross:

Employee Earthquake Preparedness for the Workplace and Home. American Red Cross, 1988. 12 pp. ($1.00 from your local Red Cross Office or by mail from Red Cross Disaster Services, 1550 Sutter Street, San Francisco, CA 94109)

Safety and Survival in an Earthquake. American Red Cross, 1989. 52 pp. ($3.00 from you local Red Cross Office or by mail from American Red Cross, Los Angeles Chapter, 2700 Wilshire Boulevard, Los Angeles, CA 90057, $3.00 plus $1.00 postage and handling)

The Emergency Survival Handbook. American Red Cross, 1989. 63 pp. ($3.00 from you local Red Cross Office or by mail from American Red Cross, Los Angeles Chapter, 2700 Wilshire Boulevard, Los Angeles, CA 90057, $3.00 plus $1.00 postage and handling)

From the Association of Bay Area Governments:

An Ounce of Prevention: Strengthening Your Wood Frame House for Earthquake Safety. California Office of Emergency Services, 1993. 36 pp. (Available from ABAG, as Pub. No. P93001BAR, $3.00 plus $1.00 postage and handling)

An Ounce of Prevention (Video). California Office of Emergency Services, 1993. (Available from ABAG, as Pub. No. P93002BAR, $10.00 plus $5.00 postage and handling)

Organizing Neighborhoods for Earthquake Preparedness. California Office of Emergency Services, 1993. 64 pp. (Available from ABAG, as Pub. No. P93006BAR, $4.00 plus $3.00 postage and handling)

From the Califoirnia Office of Emergency Services:

General HOME Preparedness Information Kit. (Set of leaflets covering personal preparedness, emergency supplies, foundation bolting, sheathing of cripple walls, water heater strapping, emergency food supplies.) California Office of Emergency Services, 1988. (OES, Oakland, single sets free -- phone 510-286-0873)

Home Buyer's Guide to Earthquake Hazards. California Office of Emergency Services, 1989. 13 pp. (OES, Oakland, single copies free -- phone 510-286-0873)

Reducing the Risks of Nonstructural Earthquake Damage -- A Practical Guide. Third Edition. By Wiss, Janney, Elstner Associates for FEMA, 1994. (Available from OES, Oakland, single copies free-- phone 510-296-0873)

From the California Seismic Safety Commission:

The Homeowners Guide to Earthquake Safety. 1992. Calif. Seismic Safety Commission Rpt. SSC 92-02, 28 pp. (Avail. from SSC, 1900 K St., Suite 100, Sacramento, CA 95814, $2.25)

From the U.S. Geological Survey:

Reducing Losses from Earthquakes through Personal Preparedness. By W.J. Kockelman, 1984. U.S. Geological Survey Open-File Report 84-765, 21 pp. (USGS, $2.75)

As a school or business owner or worker:

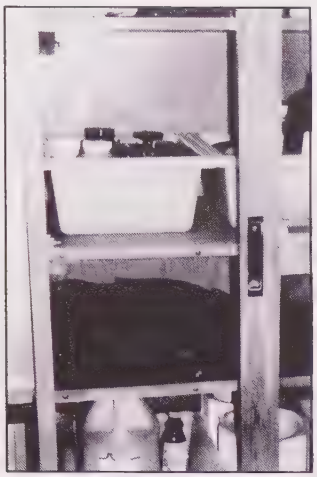

Businesses should improve their knowledge by conducting:
audits of general earthquake vulnerability; and

- risk assessments to point out ways to avoid risk through avoiding areas problem soils/geologic conditions, use of "buffer" zones around hazard areas, and hazardous materials inventory control.

Schools and businesses can mitigate risk by :

- use of specially-designed shelving systems or containers;
- use of special structural designs for buildings, tanks and pipeline supports;
- use of seismic restraints on suspended ceilings, light fixtures, equipment computer floors (such as bracing, anchors, and straps); and
- control of hazardous materials risk through secondary containment chemical isolation and separation of incompatible chemicals.

Mitigation measures can be improved. Requirements in OSHA standards and Uniform Building Code are minimums. Just because you cannot push someth over easily does not mean that the heavy object will not topple, causing injurie

- Cupboard doors (including sliding doors) can open during earthquakes. They should be fitted with positive latches.
- 1" to 1-1/2" shelf lips may not be adequate to restrain chemical reagent bottles in violent ground shaking. Lip designers should look at the size and shape of what is on the shelf.
- Some shelf anchors can fail. They should be designed to restrain full, rat than empty, shelves.
- Tanks and pipelines can have problems due to inadequate attention to det For example, anchoring thin-walled tanks may make leakage more likely contributing to the puncturing of the vessel. Proper detailing is essential.
- Gas cylinders cause problems. For example, C-clamp restraints for gas cylinders can slip off lab benches. They can slip out from under single chains. Cylinders in use should be anchored with two chains (one high, one low).

Emergency capabilities should be improved and maintained:

- use back-up systems for power, communications and water;
- improve evacuation routes through (1) avoiding placing shelving in major corridors, (2) reducing the risk of window breakage, and (3) structural retr of exit areas;
- improve the usefulness of emergency personnel through (1) training of spe response and inspection teams, (2) anchoring furniture and equipment in t offices; and (3) using databases to track those personnel and their traini and
- develop emergency response and warning systems.

Employee training programs are essential. If not trained, employees can be very "innovative" in defeating mitigation -- and in designing inadequate solutions. As many employees as possible should be trained in first aid, CPR and fire safety. Drills should be held to exercise the emergency response plan on a regular basis.

For More Information ...

From the American Red Cross:

Employee Earthquake Preparedness for the Workplace and Home. American Red Cross, 1988. 12 pp. ($1.00 from you local Red Cross Office or by mail from Red Cross Disaster Services, 1550 Sutter Street, San Francisco, CA 94109)

From the Association of Bay Area Governments for Businesses and Hospitals:

Business Resumption Planning Guidelines. California Office of Emergency Services, 1993. 28 pp. (Available from ABAG, as Pub. No. P93008BAR, $5.00 plus $2.00 postage and handling)

Earthquake Preparedness Guidelines for Hospitals. California Office of Emergency Services, 1987. 151 pp. (Available from ABAG, as Pub. No. P88001BAR, $10.00 plus $3.00 postage and handling)

Earthquake Preparedness Training for Businesses. California Office of Emergency Services, 1990. 88 pp. (Available from ABAG, as Pub. No. P90001BAR, $25.00 plus $5.00 postage and handling)

Hazardous Materials Problems in Earthquakes: A Guide to Their Cause and Mitigation. By J.B. Perkins, E. Wyatt, J.H. Schmidt, and G. Selvaduray, 1990. ABAG, 72 pp. (Available from ABAG as Pub. No. P90002EQK, $12.00 plus $3.00 postage and handling)

Toxic Gas Releases in Earthquakes: Existing Programs, Sources and Mitigation Strategies. By J.B. Perkins, E. Wyatt, and G. Selvaduray, 1991. ABAG for the South Coast Air Quality Management District, 374 pp. (Available from ABAG as Pub. No. P91002EQK, $20.00 plus $5.00 postage and handling)

From the Association of Bay Area Governments for Schools and Childcare Providers:

Earthquake Preparedness Activities for Child-Care Providers. California Office of Emergency Services, 1989. 54 pp. (Available from ABAG, as Pub. No. P89002BAR, $8.00 plus $2.00 postage and handling)

Earthquake Preparedness: What Every Childcare Provider Should Know (Video). California Office of Emergency Services, 1993. (Available from ABAG, as Pub. No. P93003BAR, $10.00 plus $5.00 postage and handling)

Earthquake Ready: Preparedness Planning for Schools. California Office of Emergency Services, 1990. 76 pp. (Available from ABAG, Pub. No. P90002BAR, $7.00 plus $3.00 postage and handling)

From the California Office of Emergency Services:

Reducing the Risks of Nonstructural Earthquake Damage -- A Practical Guide. Third Edition. By Wiss, Janney, Elstner Associates for FEMA, 1994. (Available from OES, Oakland, single copies free-- phone 510-296-0873)

From the California Seismic Safety Commission:

The Commercial Property Owners Guide to Earthquake Safety. 1993. Calif. Seismic Safety Commission Rpt. SSC 93-01, 32 pp. (Avail. from SSC, 1900 K St., Suite 100, Sacramento, CA 95814, $3.25)

As a local government elected official or staff member:

The local agency is in the forefront because local government is at the action level and earthquakes do provide action.

James E. McCarty, 1986, former Oakland Public Works Director

Large variations in the level of ground shaking hazard exist in the San Francisco Bay Area. Thus, local government programs dealing with earthquake hazards should recognize these differences.

Mitigation options include:

- land use/zoning controls, particularly for critical or hazardous facilities;
- requirements for soils and geotechnical studies;
- special building design requirements;
- special requirements for nonstructural components;
- hazardous building retrofitting and abatement programs;
- programs to strengthen housing;
- special requirements related to hazardous materials;
- infrastructure and lifeline requirements;
- disclosure requirements and posting of signs;
- disaster response planning;
- reconstruction and redevelopment planning; and
- public information and education programs.

Policy statements on all of these strategies can become a part of the safety element of a jurisdiction's general plan. However, these ***general plan policies must be backed by programs, ordinances and regulations to have any meaningful impact on our safety***.

A land use control might be to avoid particular problem areas in the siting of new critical facilities, such as fire stations. Zoning controls might include restrictions on facilities handling hazardous materials "on shakier ground."

Geotechnical studies and environmental reviews in areas of strongest shaking should be required to ***be performed by licensed professionals and go beyond statements of fact to include the conclusions and recommendations for appropriate mitigation***.

Building codes should be recognized as only minimum standards. Construction supervision by a structural engineer can prove effective for critical facilities in high intensity areas. In addition, local governments should improve the qualifications and encourage specialized training and continued education for building department personnel responsible for structural review.

Although unreinforced masonry buildings have become a symbol for hazardous buildings, they are not the only potential problem. For example, many older cities are dominated by wood-frame houses over 50 years old which were built before such buildings were required to be bolted to their foundations. Cities should consider requiring bolting and strengthening when such buildings are sold or within a fixed period. Because of the large number of such buildings and limited local resources, cities may find it appropriate to target neighborhoods "on shakier ground."

The Loma Prieta quake took 17 seconds to undo 100 years of downtown evolution. It will take a decade to recover. Become more resilient. Strengthen your buildings and economy.

Charles Eadie
Assist. Planning Director
City of Watsonville

For More Information ...

From the Association of Bay Area Governments:

Earthquake Recovery: A Survival Manual for Local Government. California Office of Emergency Services, 1993. 488 pp. (Avail. from ABAG, as Pub. No. P93007BAR, $14.00 plus $6.00 postage and handling)

Earthquake Vulnerability Analysis for Local Governments. California Office of Emergency Services, 1989. 16 pp. (Avail. from ABAG, as Pub. No. P89003BAR, $4.00 plus $2.00 postage and handling)

Liability of Local Governments for Earthquake Hazards and Losses – A Guide to the Law and Its Impacts in the States of California, Alaska, Utah and Washington. By J.B. Perkins and K. Moy, 1989. ABAG, 52 pp. (Available from ABAG as Pub. No. P88003PLN, $12.00 plus $3.00 postage and handling)

Putting Seismic Safety Policies to Work. By M. Blair-Tyler and P.A. Gregory, 1988. California Office of Emergency Services, 44 pp. (Available from ABAG, as Pub. No. P88006BAR, $9.00 plus $2.00 postage and handling)

Seismic Retrofit Incentive Programs-A Handbook for Local Government. By D. Barzel and W. Darragh, ABAG, for the California Office of Emergency Services, 1992. 252 pp. (Avail. from ABAG, as Pub. No. P92001BAR, $20.00 plus $5.00 postage and handling)

From the California Office of Emergency Services:

Reducing the Risks of Nonstructural Earthquake Damage – A Practical Guide. Third Edition. By Wiss, Janney, Elstner Associates for FEMA, 1994. (Available from OES, Oakland, single copies free– phone 510-296-0873)

From the California Seismic Safety Commission:

California at Risk–Steps to Earthquake Safety for Local Governments. By G.G. Mader and M. Blair-Tyler, 1988. Ca. Seis. Safety Comm. Rpt. SSC88-01, 92 pp. (Avail. from SSC, Sacramento, $10)

From the U. S. Geological Survey:

Geologic Principles for Prudent Land Use – A Decisionmaker's Guide for the San Francisco Bay Region. By R.D. Brown and W.J. Kockelman, 1983. U.S. Geological Survey Professional Paper 946, 97 pp. (Available from USGS, $5.50)

Look Before You Build–Requiring Geologic Studies for Reviewing Building Projects. By M. Blair Tyler, Spangle Associates, 1995. U.S. Geological Survey Circular 1130, 59 pp. (Available from USGS, free of charge)

Seismic Safety and Land Use Planning – Selected Examples from California. By M.L. Blair and W.E. Spangle, 1979. U.S. Geol. Survey Prof. Paper 941-B, 82 pp. (Available from USGS, $6.50)

WHAT'S NEXT -- OUR FUTURE PLANS ...

We continue to learn more about the ground shaking hazard. Further study of the damage patterns in the 1994 Northridge earthquake should contribute more to our knowledge of thrust faulting and the role of directivity. Further study of the 1995 earthquake in Kobe, Japan should help us confirm the role of directivity in strike-slip earthquakes. It may also help to reduce the discrepancy between the revised model used in this report and the attenuation curve calculated from 1906 data for distances within a mile of the surface trace of the fault. (See Ref. 28.) Finally, study of seismic records from these two earthquakes and the 1992 Landers earthquake should provide instrumental evidence on the role of directivity and the appropriateness of the scaling factors being used in this report.

Nature is always right – try harder to understand it.

John Blume, a "grandfather" of earthquake engineering

Two types of maps published in the 1987 version of this document have not been regenerated at this time: maximum intensity (using the highest intensity from any of the individual earthquake scenario maps) and composite risk maps (adding the individual earthquake scenario maps together based on how often the earthquakes are expected to occur and damage characteristics for three "average" building designs). Both of these types of maps need to incorporate information on the hazard from thrust faulting that is not available at this time. In addition, the probability of future earthquakes occurring is critical in any risk mapping. These probabilities are currently only available for a few of the scenarios examined. Finally, additional damage information tied to these intensities should become available during the next several months. We anticipate adding these additional maps to this document in one to two years.

ABAG is also in the process of using these intensity maps to model the expected number of housing units to be "red tagged" by local building departments as "unsafe for occupancy" in each of the scenarios depicted on the following pages. Although the table on page 20 provides an "official" definition for the various categories of shaking intensity, the following table predicting the percentage of single-family homes expected to be "red tagged" also provides sobering data.

TABLE: PERCENT OF DWELLING UNITS RED TAGGED

TYPE	MODIFIED MERCALLI INTENSITY					
	V	VI	VII	VIII	IX	X+
Mobile Home	0.0	0.0	0.4	12.0	76.0	86.0
Wood-Frame, 1-3 Stories, <1940, Single Family	0.0	0.0	0.11	3.0	18.0	20.0
Wood-Frame, 1-3 Stories, >1939, Single Family	0.0	0.0	0.0	0.18	7.5	10.0

Note: The "0" values provided in these tables are actually greater than zero, but still quite small. Although occasional dwellings are "tagged" in these categories, there are also large numbers of dwellings exposed to these relatively low levels of shaking. The values are based on statistics from several earthquakes. In the 1989 Loma Prieta earthquake, over one-third of the pre-1940 single-family homes exposed to modified Mercalli intensity IX-X+ were "red tagged."

To make your home as safe as one built after 1940, bolt the home to the foundation and brace the "cripple" wall (the wall between the foundation and the floor joists)! Similarly, the installation of "earthquake bracing" to your mobile home will greatly reduce the chances of it falling from its supports.

SHAKING INTENSITY MAP PLATES ...

The following twelve maps show modeled shaking intensity. The maps show the hazard using the modified Mercalli intensity scale. The full description of each intensity level is provided in the Table below. Note that this full description has been shortened to one to two key words on the maps themselves due to space constraints. Please read the full description of each intensity level to ensure a better understanding of the shaking expected. We also recommend reading the documentation on how these maps were prepared on pages 4-9 before using the maps.

TABLE -- MODIFIED MERCALLI INTENSITY SCALE

MMI Value	Summary Damage Description Used on Maps	**Full Description** (from Ref. 40)
I.		Not felt. Marginal and long period effects of large earthquakes.
II.		Felt by persons at rest, on upper floors, or favorably placed.
III.		Felt indoors. Hanging objects swing. Vibration like passing of light trucks. Duration estimated. May not be recognized as an earthquake.
IV.		Hanging objects swing. Vibration like passing of heavy trucks; or sensation of a jolt like a heavy ball striking the walls. Standing motor cars rock. Windows, dishes, doors rattle. Glasses clink. Crockery clashes. In the upper range of IV wooden walls and frame creak.
V.	**Pictures Move**	Felt outdoors; direction estimated. Sleepers wakened. Liquids disturbed, some spilled. Small unstable objects displaced or upset. Doors swing, close, open. Shutters, pictures move. Pendulum clocks stop, start, change rate.
VI.	**Objects Fall**	Felt by all. Many frightened and run outdoors. Persons walk unsteadily. Windows, dishes, glassware broken. Knickknacks, books, etc., off shelves. Pictures off walls. Furniture moved or overturned. Weak plaster and masonry D cracked. Small bells ring (church, school). Trees, bushes shaken (visibly, or heard to rustle).
VII.	**Nonstructural Damage**	Difficult to stand. Noticed by drivers of motor cars. Hanging objects quiver. Furniture broken. Damage to masonry D, including cracks. Weak chimneys broken at roof line. Fall of plaster, loose bricks, stones, tiles, cornices (also unbraced parapets and architectural ornaments). Some cracks in masonry C. Waves on ponds; water turbid with mud. Small slides and caving in along sand or gravel banks. Large bells ring. Concrete irrigation ditches damaged.
VIII.	**Moderate Damage**	Steering of motor cars affected. Damage to masonry C; partial collapse. Some damage to masonry B; none to masonry A. Fall of stucco and some masonry walls. Twisting, fall of chimneys, factory stacks, monuments, towers, elevated tanks. Frame houses moved on foundations if not bolted down; loose panel walls thrown out. Decayed piling broken off. Branches broken from trees. Changes in flow or temperature of springs and wells. Cracks in wet ground and on steep slopes.
IX.	**Heavy Damage**	General panic. Masonry D destroyed; masonry C heavily damaged, sometimes with complete collapse; masonry B seriously damaged. (General damage to foundations.) Frame structures, if not bolted, shifted off foundations. Frames racked. Serious damage to reservoirs. Underground pipes broken. Conspicuous cracks in ground. In alluvial areas sand and mud ejected, earthquake fountains, sand craters.
X.	**Extreme Damage**	Most masonry and frame structures destroyed with their foundations. Some well-built wooden structures and bridges destroyed. Serious damage to dams, dikes, embankments. Large landslides. Water thrown on banks of canals, rivers, lakes, etc. Sand and mud shifted horizontally on beaches and flat land. Rails bent slightly.
XI.		Rails bent greatly. Underground pipelines completely out of service.
XII.		Damage nearly total. Large rock masses displaced. Lines of sight and level distorted. Objects thrown into the air.

Masonry A: Good workmanship, mortar, and design; reinforced, especially laterally, and bound together by using steel, concrete, etc.; designed to resist lateral forces.

Masonry B: Good workmanship and mortar; reinforced, but not designed in detail to resist lateral forces.

Masonry C: Ordinary workmanship and mortar; no extreme weaknesses like failing to tie in at corners, but neither reinforced nor designed against horizontal forces.

Masonry D: Weak materials, such as adobe; poor mortar; low standards of workmanship; weak horizontally.

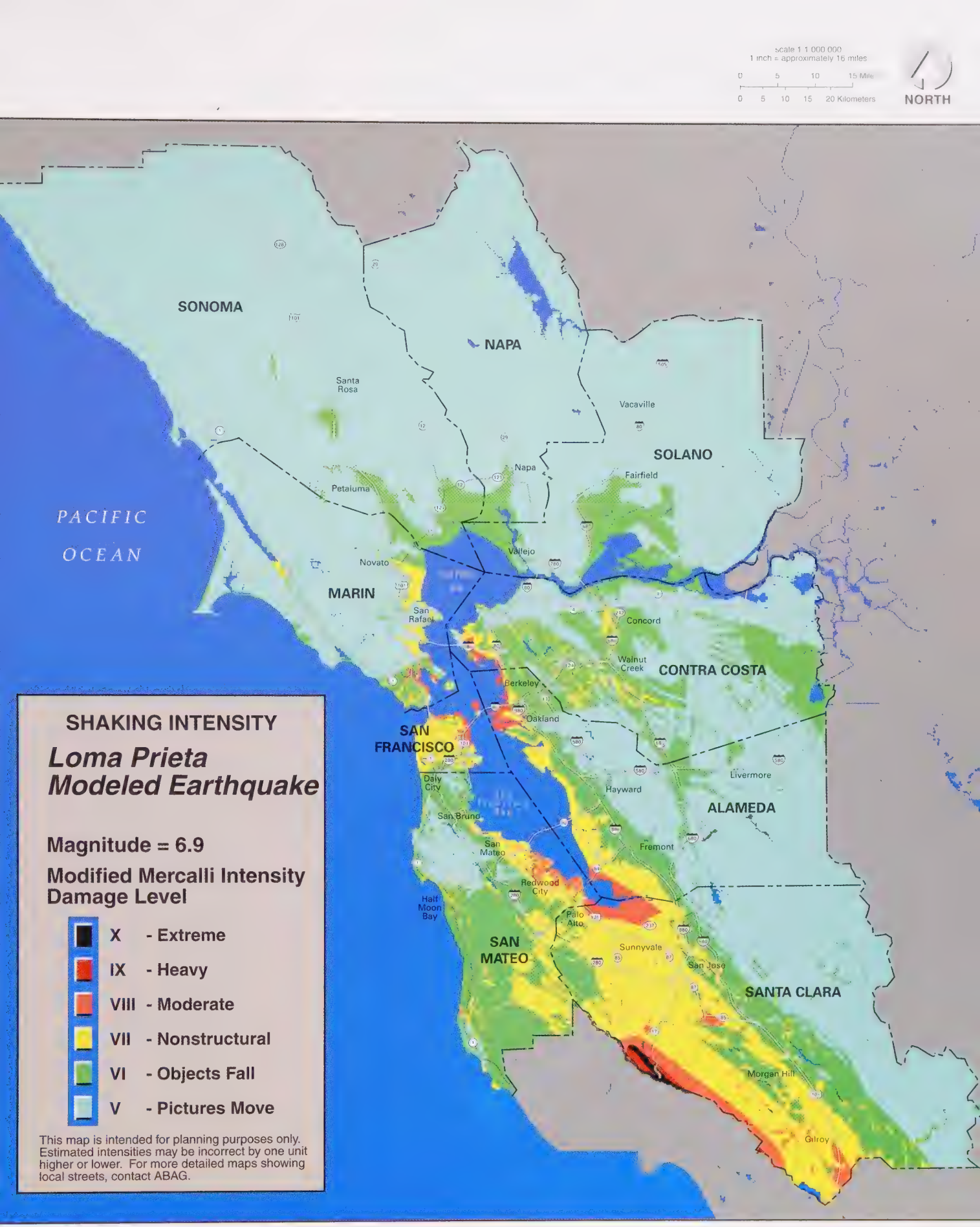

Source: *On Shaky Ground* – 1995

ABAG©
Association of Bay Area Governments

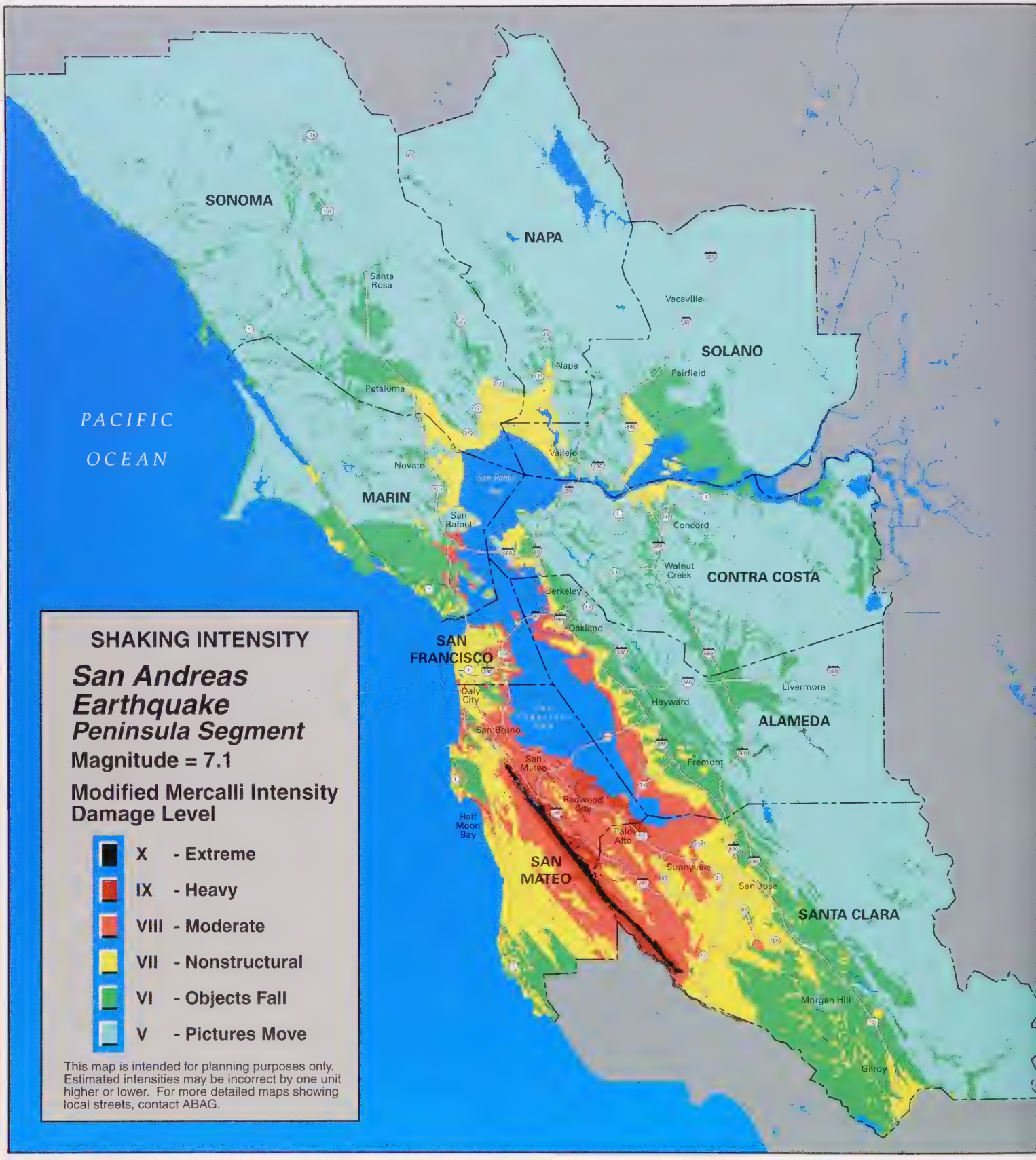

Source: *On Shaky Ground* – 1995

ABAG©
Association of Bay Area Governments

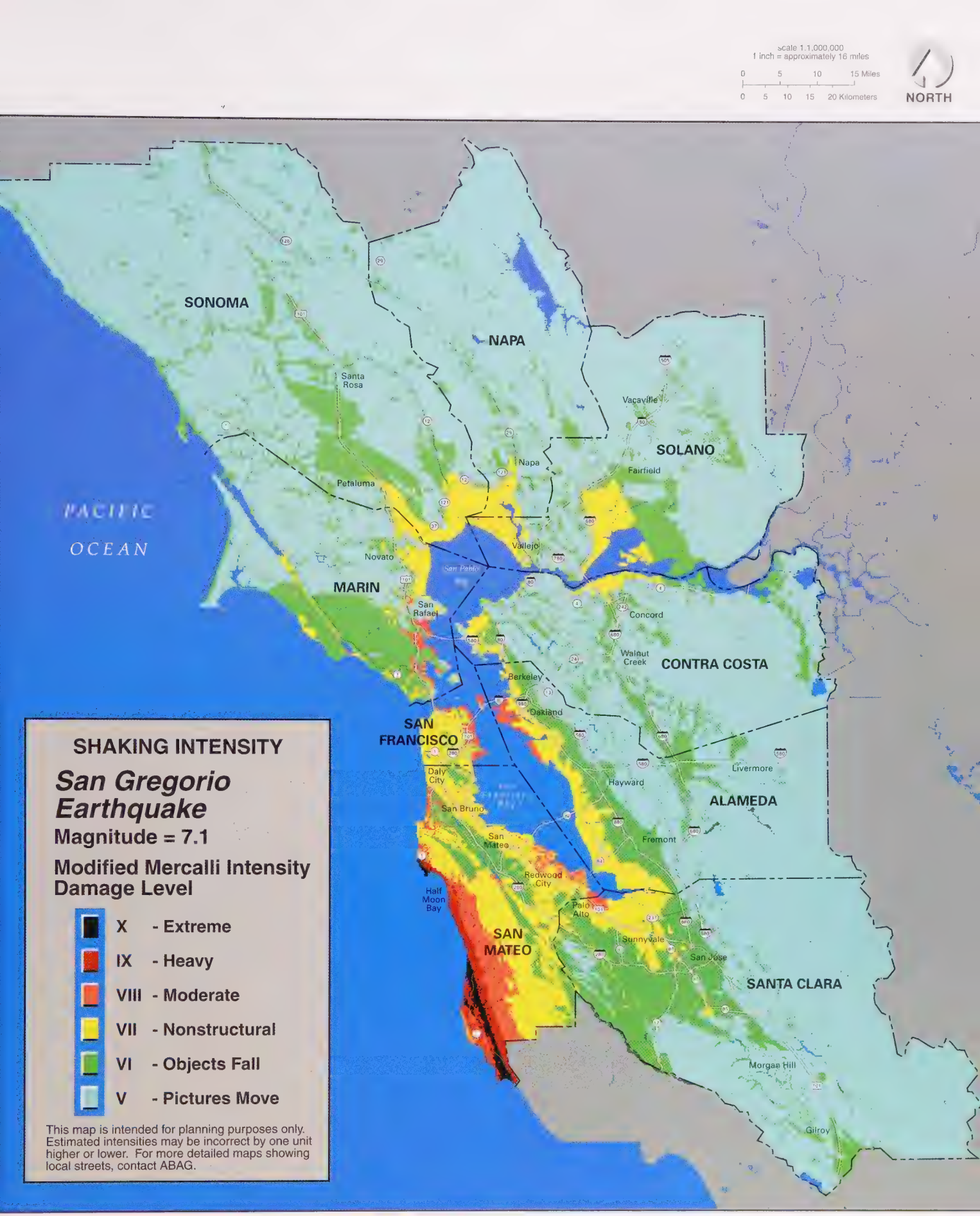

Source: *On Shaky Ground* – 1995

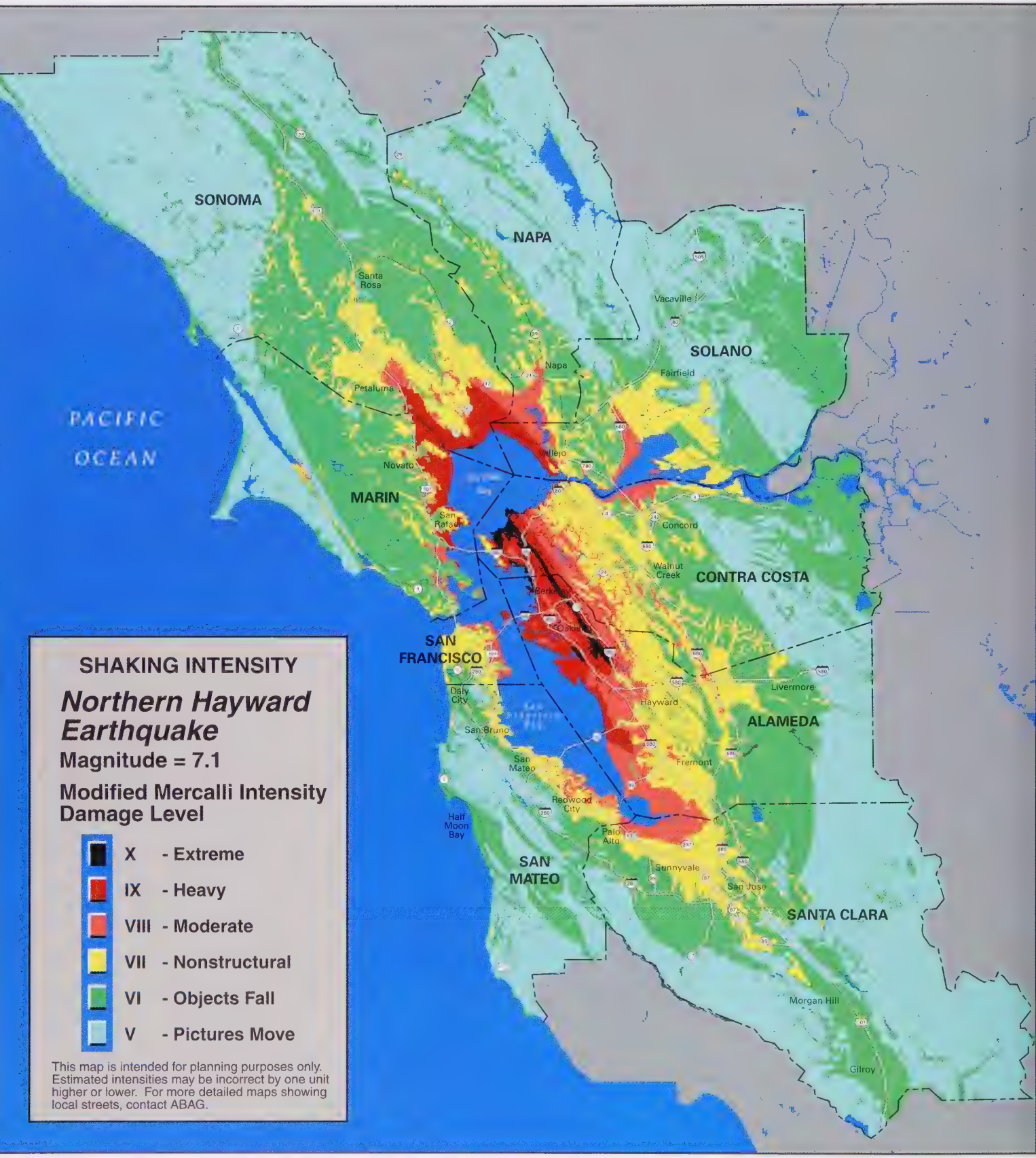

Source: *On Shaky Ground* – 1995

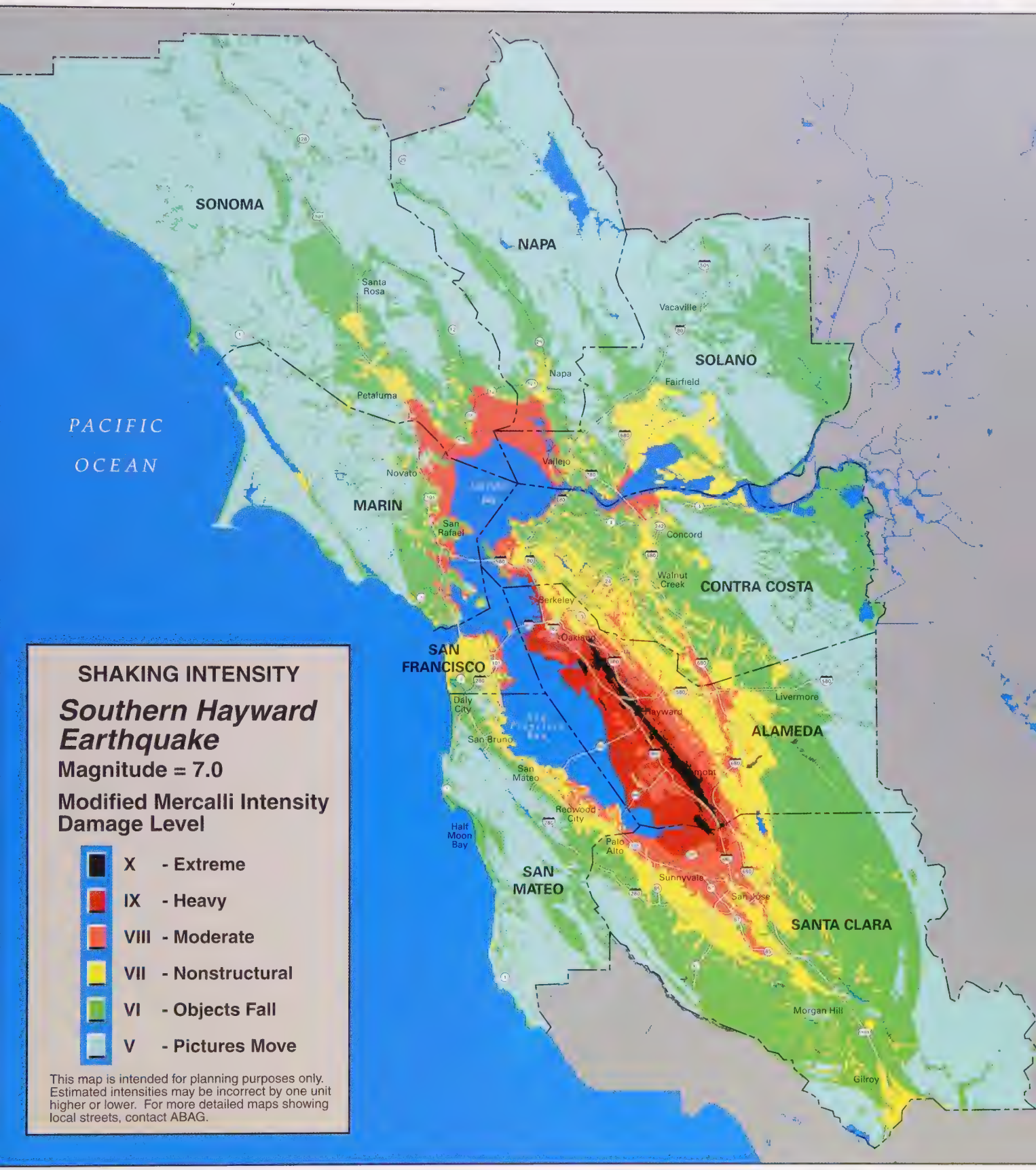

Source: *On Shaky Ground* – 1995

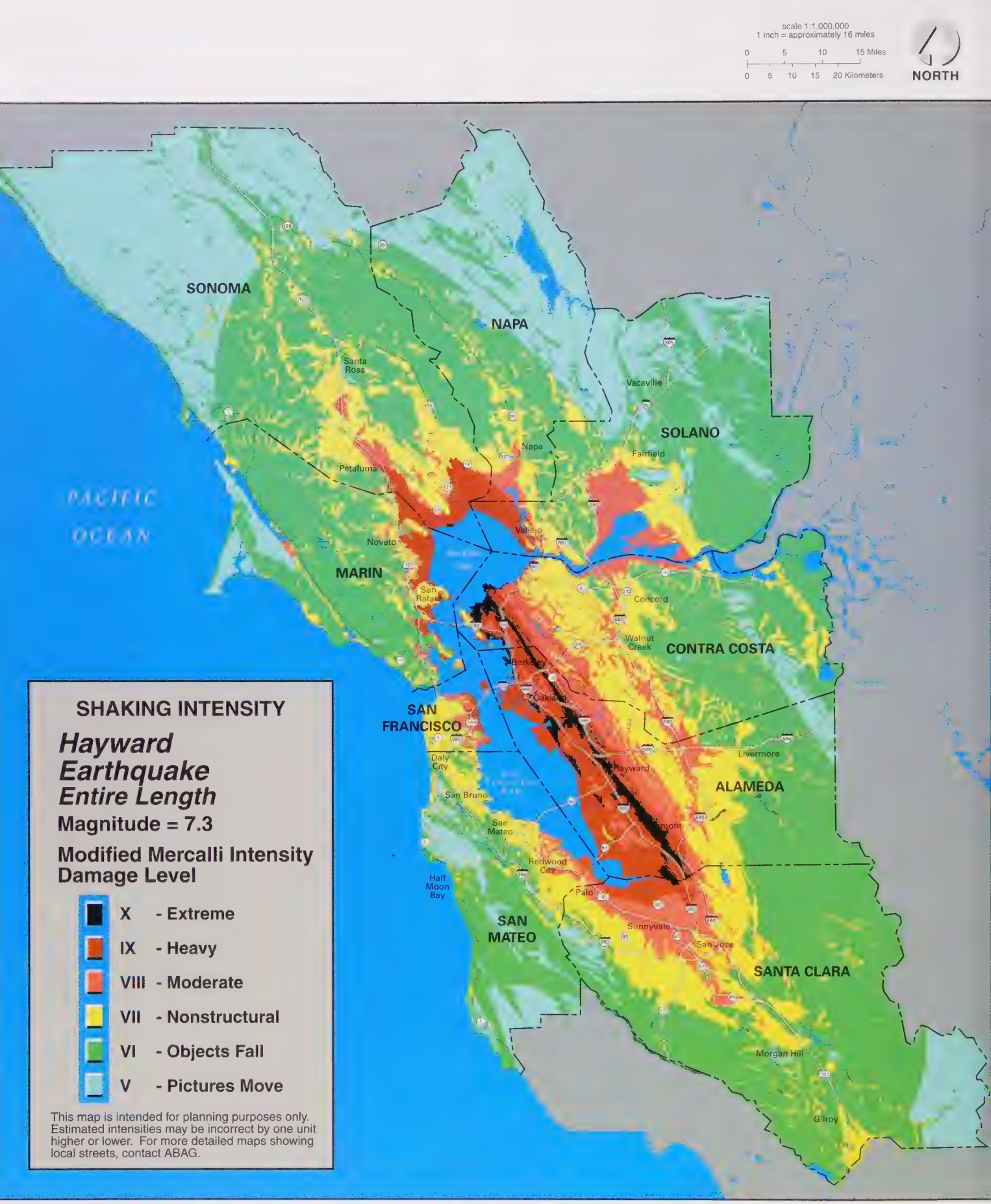

Source: *On Shaky Ground* – 1995

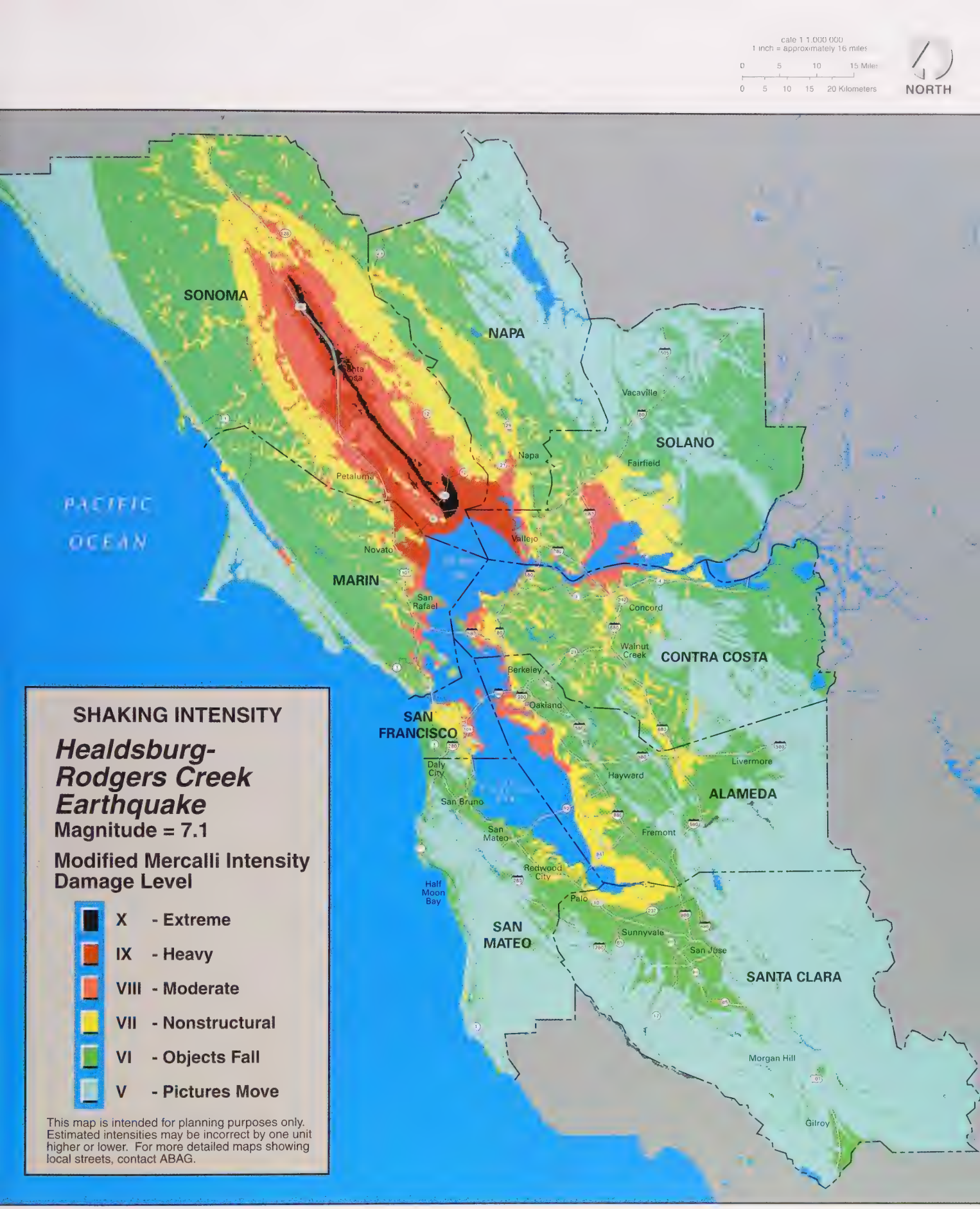

Source: *On Shaky Ground* – 1995

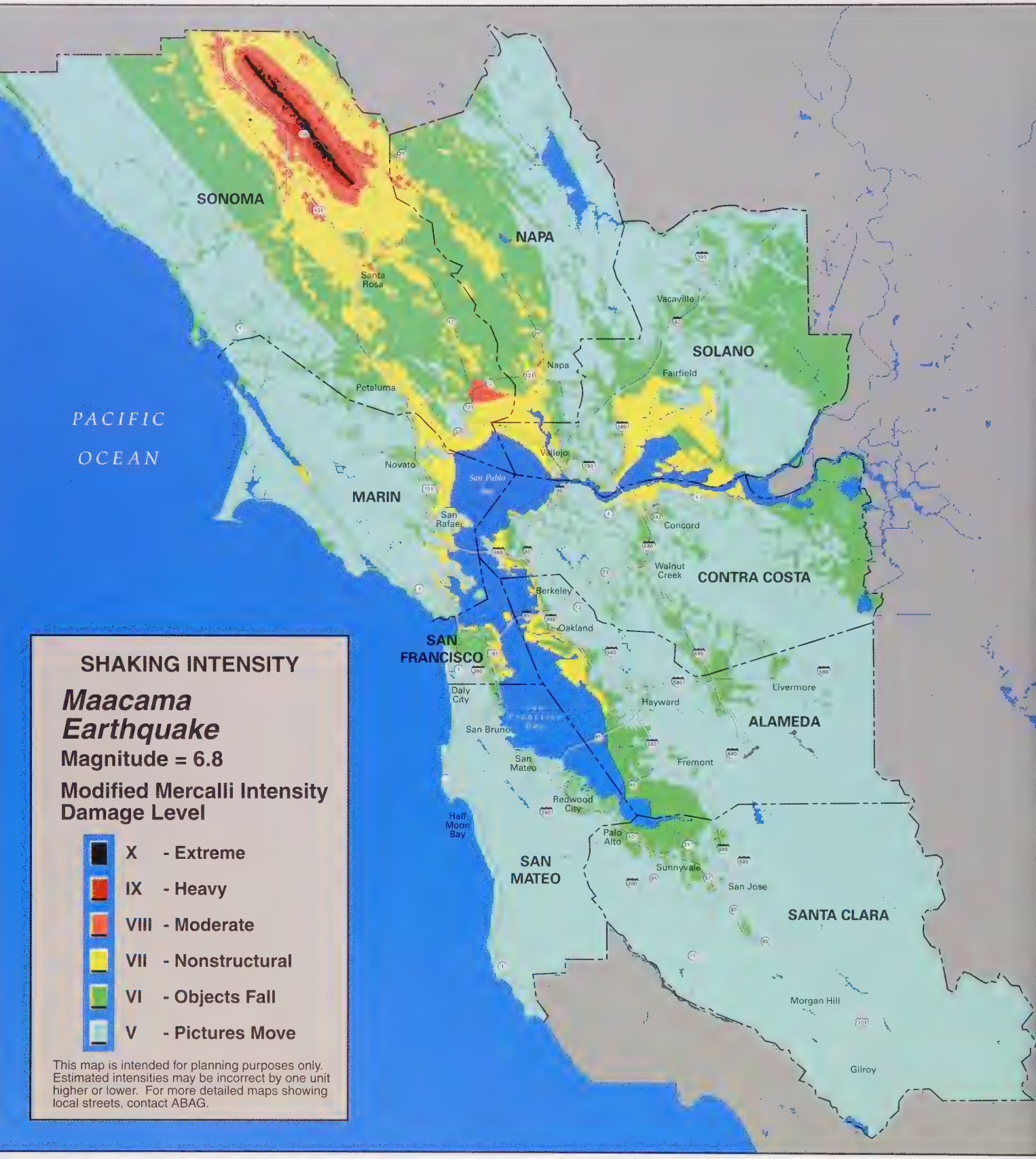

Source: *On Shaky Ground* – 1995

ABAG©
Association of Bay Area Governments

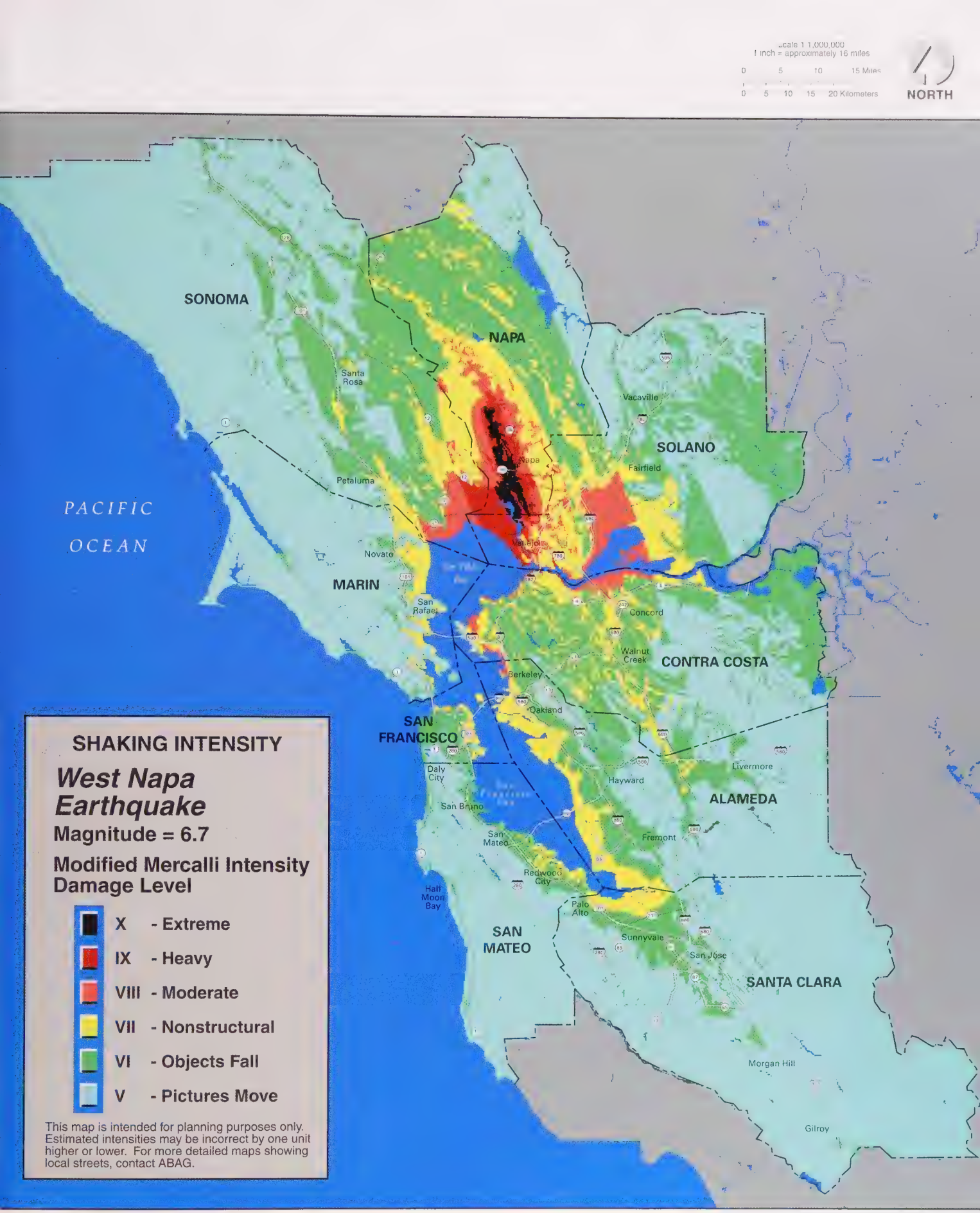

Source: *On Shaky Ground* – 1995

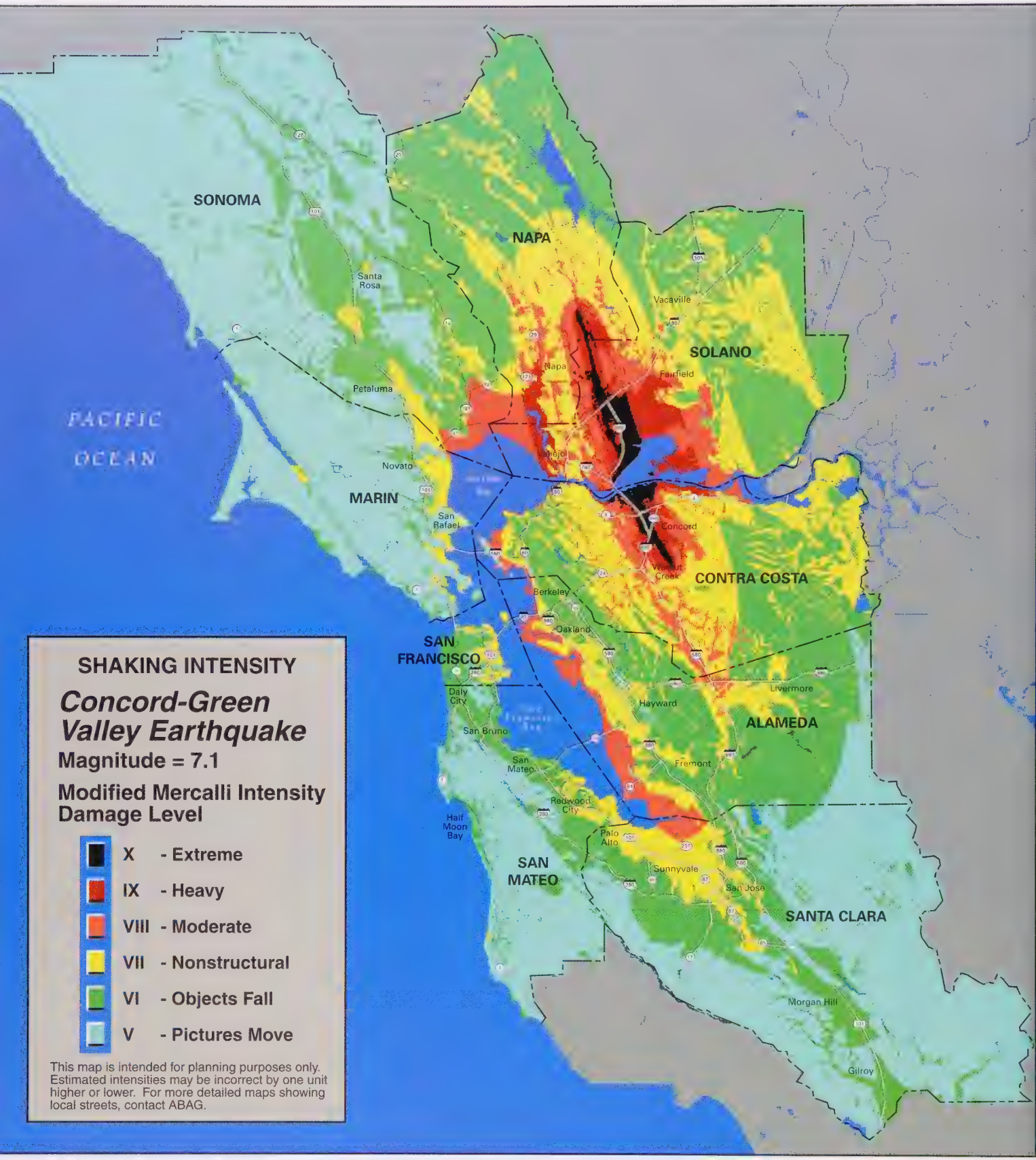

Source: *On Shaky Ground* – 1995

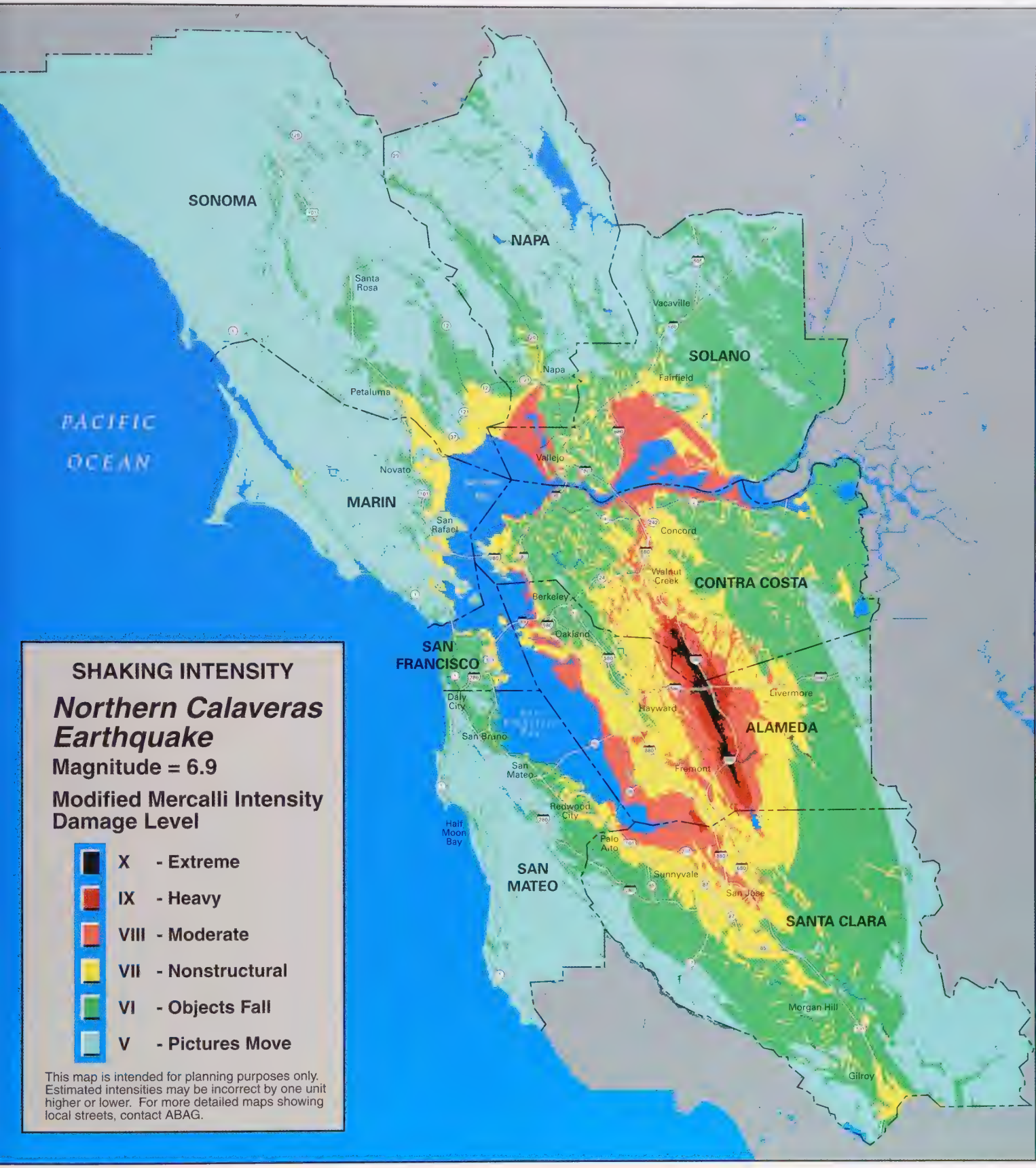

Source: *On Shaky Ground* – 1995

ABAG©
Association of Bay Area Governments

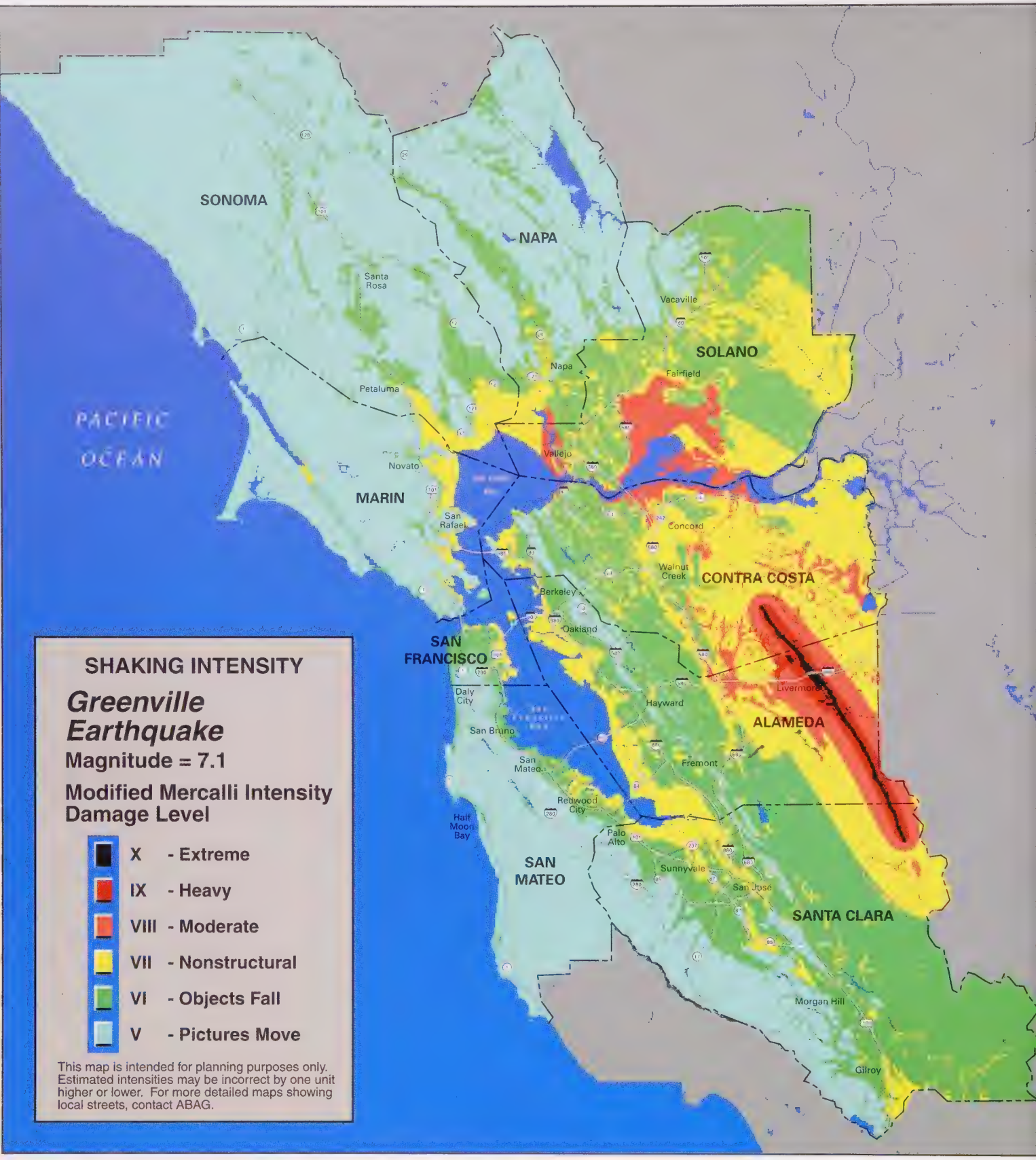

Source: *On Shaky Ground* – 1995

ABAG©
Association of Bay Area Governments

REFERENCES ...

Sources of Fault Location and Activity Data

1. California Division of Mines and Geology, varies. ***Fault Special Studies Zones Maps*** for selected 7.5' quadrangles in the San Francisco Bay Area: California Division of Mines and Geology.

2. Helley, E.J., and Herd, D.G., 1977. ***Faults with Quaternary Displacement - Northeastern San Francisco Bay Region, California***: U.S. Geological Survey Misc. Field Studies Map MF-881.

3. Working Group on California Earthquake Probabilities, 1990. ***Probabilities of Large Earthquakes in the San Francisco Bay Region, California***: U.S. Geological Survey Circular 1053, 51 pp.

4. Working Group on California Earthquake Probabilities, 1988. ***Probabilities of Large Earthquakes Occurring in California on the San Andreas Fault***: U.S. Geological Survey Open-File Report 88-398.

Sources of Geologic Data

The following maps were converted to digital form (digitized) by ABAG staff from 1977 to 1983. Staff working on this effort included Malcolm Gilmour, Roberta Moreland, Ruth Robinson and Paula Shultz.

5. Blake, Jr., M.C., Bartow, J.A., Frizzell, Jr., V.A., Schlocker, J., Sorg, D., Wentworth, C.M., and Wright, R.H., 1974. ***Preliminary Geologic Map of Marin and San Francisco Counties and Parts of Alameda, Contra Costa and Sonoma Counties, California***: U.S. Geological Survey Misc. Field Studies Map MF-574 (SFBRS Basic Data Contribution 64).

6. Blake, Jr., M.C., Smith, J.T., Wentworth, C.M., and Wright, R.H., 1971. ***Preliminary Geologic Map of Western Sonoma County and Northern Marin County, California***: U.S. Geological Survey Open-File Map (SFBRS Basic Data Contribution 12).

7. Bonilla, M.G., 1971. ***Preliminary Geologic Map of the San Francisco South Quadrangle and Part of the Hunters Point Quadrangle, California***: U.S. Geological Survey Misc. Field Studies Map MF-311 (SFBRS Basic Data Contribution 29).

8. Brabb, Earl E., 1970. ***Preliminary Geologic Map of the Central Santa Cruz Mountains, California:*** U.S. Geological Survey Open-File Map (SFBRS Basic Data Contribution 6).

9. Brabb, Earl E., unpublished. Personal communication on the geology of the Newark and San Leandro Quadrangles, California.

10. Brabb, E.E., and Dibblee, Jr., T.W., 1978 to 1980. ***Preliminary Geologic Maps of Selected Quadrangles in Southwestern Santa Clara County, California***: U.S. Geological Survey Open-File Reports (Castle Rock Ridge - 79-659; Los Gatos - 78-453; Santa Teresa Hills - unpublished; Laurel - 78-84; Loma Prieta - 80-944; Watsonville East and Chittenden - 78-453).

11. Brabb, E.E., and Pampeyan, E.H., 1983. ***Geologic Map of San Mateo County, California***: U.S. Geological Survey Misc. Investigations Map I-1257-A.

12. Brabb, E.E., Sonneman, H.S., and Switzer, Jr., J.R., 1971. ***Preliminary Geologic Map of the Mount Diablo-Byron Area, Contra Costa, Alameda and San Joaquin Counties, California***: U. S. Geological Survey Open-File Map (SFBRS Basic Data Contribution 28).

13. Burke, D.B., Helley, E.J., Lajoie, K.R., Tinsley, J.C., and Weber, G.E., 1979. ***Geologic Map of the Flatlands Deposits of the San Francisco Bay Region***: U.S. Geological Survey Professional Paper 944, 88 pp.

14. Cotton, W.R., 1972. ***Preliminary Geologic Map of the Franciscan Rocks in the Central Part of the Diablo Range, Santa Clara and Alameda Counties, California***: U.S. Geological Survey Misc. Field Studies Map MF-343 (SFBRS Basic Data Contribution 39).

15. Dibblee, Jr., T.W., 1972 to 1981. ***Preliminary Geological Maps of Selected Quadrangles, Alameda, Contra Costa and Santa Clara Counties, California:*** U.S. Geological Survey Open-File Reports.

16. Fox, Jr., K.F., Sims, J.D., Bartow, J.A., and Helley, E.J., 1973. ***Preliminary Geologic Map of Eastern Sonoma County and Western Napa County, California***: U.S. Geological Survey Misc. Field Studies Map MF-483 (SFBRS Basic Data Contribution 56).

17. Radbruch, D.H., 1957. ***Areal and Engineering Geology of the Oakland West Quadrangle, California***: U.S. Geological Survey Misc. Geologic Investigations Map I-239.

18. Radbruch, D.H., 1969. ***Areal and Engineering Geology of the Oakland East Quadrangle, California***: U.S. Geological Survey Geological Quadrangle Map of the United States Map GQ-679.

19. Schlocker, J., Bonilla, M.G., and Radbruch, D.H., 1958. ***Geology of the San Francisco North Quadrangle, California***: U.S. Geological Survey Misc. Geologic Investigations Map I-272.

20. Sims, J. D., Fox, Jr., K.F., Barlow, J.A., Helley, E.J., 1973. ***Preliminary Geologic Map of Solano County and parts of Napa, Contra Costa, Marin and Yolo Counties, California***: U.S. Geological Survey Misc. Field Studies Map MF-484 (SFBRS Basic Data Contribution 54).

Other References Cited

21. Ben-Menahem, A., 1961. "Radiation of Seismic Surface Waves from Finite Moving Sources," *in* ***Bulletin of the Seismological Society of America***, v 51, pp. 401-435.

22. Beroza, G.C., and P. Spudich, 1988. "Linearized inversion for fault rupture behavior: application to the 1984 Morgan Hill, California, Earthquake," *in* ***Journal of Geophysical Research***, v. 93, pp. 6275-6296.

23. Boatwright, J., 1982. "A Dynamic Model for Far-Field Acceleration," *in* ***Bulletin of the Seismological Society of America***, v. 72, pp. 1049-1068.

24. Boatwright, J., and Boore, D.M., 1982. "Analysis of the Ground Accelerations Radiated by the 1980 Livermore Valley Earthquakes for Directivity and Dynamic Source Characteristics" *in* ***Bulletin of the Seismological Society of America***, v. 72, no. 6, pp 1843-1865.

25. Boore, D.M., Joyner, W.B., and Fumal, T.E., 1993. ***Estimation of Response Spectra and Peak Accelerations from Western North American Earthquakes: An Interim Report***: U.S. Geological Survey Open-File Report 93-509, Denver, CO.

26. Borcherdt, R.D., 1994. "Estimates of Site-Dependent Response Spectra for Design (Methodology and Justification)" *in* ***Earthquake Spectra*** (November 1994): Earthquake Engineering Research Institute (EERI), Oakland, v. 10, no.4, pp. 617-653.

27. Borcherdt, R.D., Gibbs, J.F., and Fumal, T.E., 1978. "Progress on Ground Motion Predictions for the San Francisco Bay Region, California" *in* ***Proceedings Second International Conference on Microzonation for Safer Constr. Research, and Application***. Also, *in* ***Progress on Seismic Zonation in the San Francisco Bay Region***: U.S. Geological Survey Circular 807, pp. 13-25. (The Circular contains a series of eight papers from that Conference that were presented together as a set.)

28. Borcherdt, R.D., Gibbs, J.F., and Lajoie, K.R., 1975. ***Maps Showing Maximum Earthquake Intensity Predicted for Large Earthquakes on the San Andreas and Hayward Faults***: U.S. Geological Survey Misc. Field Studies Map MF-709, Scale 1:125,000.

29. Borcherdt, R.D., and Glassmoyer, G., 1992. "On the Characteristics of Local Geology and Their Influence on Ground Motions Generated by the Loma Prieta Earthquake in the San Francisco Bay Area, California" *in* ***Bulletin of the Seismological Society of America***, v. 82, no. 2.

30. California Division of Mines and Geology (CDMG), 1990. McNutt, S.R., and Sydnor, R.H., ed., ***The Loma Prieta (Santa Cruz Mountians), California, Earthquake of 17 October 1989***: CDMG Special Publication 104, Sacramento, 142 pp.

31. Das, S., and Scholz, C.H., 1983. "Why Large Earthquakes Do Not Nucleate at Shallow Depths" *in* ***Nature***, v. 305, no.5935, pp. 621-623.

32. Davis, J.F., Bennett, J.H., Borchardt, G.A., Kahle, J.E., Rice, S.J., and Silva, M.A., 1982. ***Earthquake Planning Scenario for a Magnitude 8.3 Earthquake on the San Andreas Fault in the San Francisco Bay Area***: California Division of Mines and Geology Special Publication 61, Sacramento, 160 pp.

33. Evernden, J.F., 1991. ***Computer Programs and Databases Useful for Prediction of Ground Motion Resulting from Earthquakes in California and the Coterminous United States***: U.S. Geological Survey Open-File Report 91-338, Denver, CO.

34. Evernden, J.F., Kohler, W.M., and Clow, G.D., 1981. ***Seismic Intensities of Earthquakes of Conterminous United States – Their Prediction and Interpretation***: U.S. Geological Survey Professional Paper 1223, 56 pp.

35. Evernden, J.F., and Thompson, J.M., 1988. ***Predictive Model for Important Ground Motion Parameters Associated with Large and Great Earthquakes***: U. S. Geological Survey Bulletin 1838, 27 pp.

36. Fumal, T.E., 1978. ***Correlations Between Seismic Wave Velocities and Physical Properties of Near-Surface Geologic Materials in the Southern San Francisco Bay Region, California***: U.S. Geological Survey Open-File Report 78-1067, Denver, CO, 52 pp.

37. Housner, G.W, 1970. "Strong Ground Motion" *in* ***Earthquake Engineering***, R.L. Wiegel, ed., Prentice Hall, Inc., Englewood Cliffs, N.J., pp. 75-92.

38. Joyner, W.B., and Boore, D.M., 1981. 'Peak Horizontal Acceleration and Velocity from Strong Motion Records Including Records from the 1979 Imperial Valley, California Earthquake," *in* ***Bulletin of the Seismological Society of America***, v. 71, pp. 2011-2038.

39. Li , Y-G., Aki, K., Adams, D., Hasemi, A., Lee, W.H.K., 1994. 'Seismic Guided Waves Trapped in the Fault Zone of the Landers, Calif., Earthquake of 1992" *in* ***Jour. of Geophysical Reseach***, v. 99, no. 6, p. 11705.

40. Richter, C.F., 1958. ***Elementary Seismology***. W.H. Freeman and Company, San Francisco, pp. 135-149; 650-653.

41. Perkins, J.B., 1992. ***Estimates of Uninhabitable Dwelling Units in Future Earthquakes Affecting the San Francisco Bay Region.*** ABAG: Oakland, CA, 89 pp.

42. Perkins, J.B., 1987a. ***The San Francisco Bay Area–On Shaky Ground***. ABAG: Oakland, CA, 32 pp. (Earlier version of this report -- out of print.)

43. Perkins, J.B., 1987b. ***Cumulative Damage Potential from Earthquake Ground Shaking, San Mateo County, California***: U.S. Geological Survey Misc. Investigations Map I-1257-I, 17 pp. and 3 map sheets with scale 1:62,500. (Documents earlier versions of maps.)

44. Perkins, J.B., 1983. ***Using Earthquake Intensity and Related Damage to Estimate Maximum Earthquake Intensity and Cumulative Damage Potential from Earthquake Ground Shaking***: ABAG Eq. Map. Proj. Working Paper #17, Oakland, 59 pp., 20 maps at 1:250,000. (Out of print.)

45. Somerville, P.G., and Yoshimura, J., 1990. 'The Influences of Critical Moho Reflections on Strong Ground Motions Recorded in San Francisco and Oakland During the 1989 Loma Prieta Earthquake" *in* ***Geophysics Research Letters***, v. 17, pp. 1203-1206.

46. Steinbrugge, K.V., Bennett, J.H., Lagorio, H.J., Davis, J.F., Borchardt, G. and Toppozada, T.R., 1987. ***Earthquake Planning Scenario for a Magnitude 7.5 Earthquake on the Hayward Fault in the San Francisco Bay Area***: Calif. Division of Mines and Geology Sp. Pub. 78, Sacramento, 229 pp.

47. Stover, C.W., Reagor, B.G., Baldwin, F.W., and Brewer, L.R., 1990. ***Preliminary Isoseismal Map for the Santa Cruz (Loma Prieta), California, Earthquake of October 19, 1989 UTC***: U.S. Geolgocial Survey Open-File Report 90-18, Denver, CO, 24 pp.

48. Wells, D.L., and Coppersmith, K.J., 1994. 'New Empirical Relationships among Magnitude, Rupture Length, Rupture Width, Rupture Area, and Surface Displacement" *in* ***Bulletin of the Seismological Society of America***, v. 84, no. 4, pp. 974-1002.

TECHNICAL APPENDIX A-- SOURCE MODEL FOR MAPPING INTENSITIES FOR LARGE STRIKE-SLIP EARTHQUAKES

Introduction

Three aspects of earthquake sources are critical for estimating ground motions in the near and intermediate field of large strike-slip earthquakes:

- the scaling of ground motions with source size
- the finite extent of the earthquake source
- the focusing of seismic radiation, or directivity

The first aspect is the scaling of ground motion with source size, that is, how much does the ground motion increase as the size, or the magnitude, of the earthquake increases? The usual course of seismological research is to use the information from more frequent moderate earthquakes to predict the effects of rarer large earthquakes. The methods used for these extrapolations are known as scaling relations. Because there are relatively few recordings for great earthquakes, the empirical scaling relations for these earthquakes are poorly determined.

The second aspect is the effect of the physical extent of the source, or the source finiteness, on the radiated ground motions. In general, earthquakes are areally distributed, that is, an earthquake radiates seismic waves from those parts of the fault area that slip during the rupture process. The physical structure of the problem implies that ground motions must saturate, or reach a maximum, near the fault surface. However, so few recordings have been obtained near the faults of large earthquakes that this saturation cannot be readily discerned in the data (Joyner and Boore, 1981).

The third aspect is the focusing of seismic energy, or directivity, resulting from the geometry of the earthquake rupture. If we know the rupture geometry, it is possible to determine reasonable estimates of the directivity. For example, the effect of directivity for a long strike-slip earthquake can be bounded by the limiting cases of the rupture nucleating at either end. In general, however, estimating the effect of directivity for the rupture of a fault segment requires taking an expectation over the set of possible hypocenters and rupture histories.

The source model used in this report contains source scaling, source finiteness, and directivity. Although the fault is buried, the motions near the fault trace are very strong. This near-fault motion results from the combination of a partially updip rupture and the amplification of ground motion associated with the velocity structure of the fault itself. Combining this near-fault intensity with strong horizontal directivity yields a source model that fits the 1906 intensities as a function of distance from the fault trace, as well as fits the intensity patterns for the 1989 Loma Prieta and 1984 Morgan Hill earthquakes. Further work is planned during 1995 to apply this technique to earthquakes on thrust faults such as the 1994 Northridge earthquake, and to test the model using strong ground recordings of the 1995 Kobe, the 1994 Northridge, and the 1992 Landers earthquakes.

Background

To consider these three aspects of the seismic source, it is useful to discuss how they are addressed in the three source models that have been used for mapping intensity and ground motion. The three models we will discuss are the attenuation relationship determined for the 1906 earthquake by Borcherdt et al. (1975), the model and program by Evernden (1991) derived from the models and analyses in Evernden et al. (1981) and Evernden and Thompson (1988), and the source model that forms the basis for the regressions of Joyner and Boore (1981) and Boore et al. (1993). While Joyner and Boore (1981) did not make ground motion or intensity maps, their regression models for peak ground acceleration (PGA), peak ground velocity (PGV), and more recently, for the pseudo-velocity response spectra (Boore et al., 1993), have been used by other researchers to map ground motions.

Borcherdt et al. (1975) derived an attenuation law for the San Francisco intensity scale as a function of the distance normal to the San Andreas fault in the 1906 San Francisco earthquake. The set of intensities that they fit were obtained on a single rock-type, the Franciscan assemblage. Their "observed" intensities are shown in Figure 1. These researchers also estimated differences in the observed intensity between the Franciscan formation and the other surficial rock-types in the area. They then mapped the 1906 intensities, with corrections for these rock-types, as a function of distance from the San Andreas and Hayward faults, to estimate the maximum intensity expected for large earthquakes on these two faults.

Borcherdt et al. (1975) fit the intensity as a function of the inverse of the distance from the surface trace of the fault, motivated by the very large intensities observed within 2 km of the fault trace. This clustering of the strongest intensities along the fault trace clearly distinguishes their method for estimating intensity from the models of Evernden et al. (1981) and Joyner and Boore (1981) where the seismic source is buried, and expected ground motions and intensities do not peak near the fault trace.

The 1906 San Francisco earthquake approximates a limiting case for considering source finiteness, in that the 1906 rupture extends far beyond the sites in San Francisco and the Bay Area. Borcherdt et al. (1975) propose no scaling to estimate the ground motion for smaller earthquakes. There is no explicit directivity in the model because no intensities were observed beyond the ends of the 1906 faulting.

Perkins (1983, 1987a, 1987b, and 1992) has applied this attenuation in an effort to model various earthquakes that have occured or are anticipated to occur in the Bay Area, including the 1989 Loma Prieta earthquake, by using the closest distance to the rupture trace in the place of the normal distance from the fault. In the first three reports, Perkins scales the intensity by dropping each intensity by one unit for $\mathbf{M} \approx 7$ events. Perkins (1992) eliminated this scaling.

Evernden (1991) uses a set of empirical relations among fault length, magnitude, and radiated energy as his scaling relations. He subdivides his finite length source into a set of subsources and sums the radiation from these subsources using a unique summation rule. His summation procedure yields a distributed source so that the intensities saturate, that is, reach a limiting value in the near-field. His fault and its subsources are buried, so the ground motions predicted along the fault trace are moderate.

To compare Evernden's attenuation with that of Borcherdt et al. (1975), we have modeled the 1906 earthquake using the computer program of Evernden (1991) and assuming an intensity correction of $\Delta I = -2.2$, Evernden's correction for Franciscan sandstone. Evernden's predicted intensity is plotted as a shaded line. His predicted curve significantly underestimates the observed 1906 intensities within 5 km of the fault trace. This underestimate results from both the depth of Evernden's source and the lack of directivity in his model.

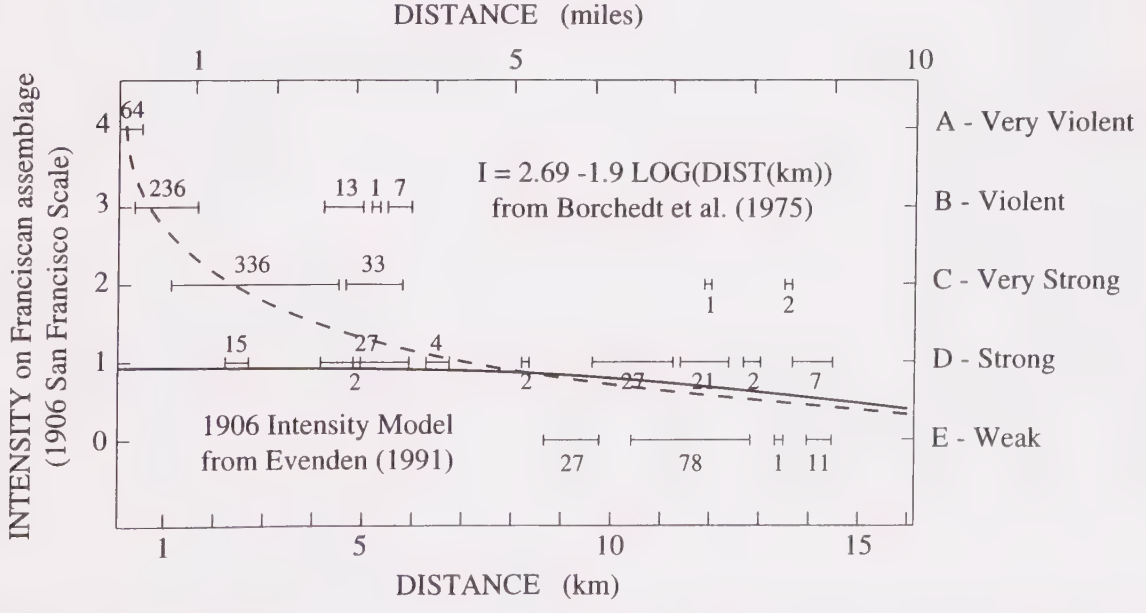

FIGURE 1. San Francisco intensity, observed at sites on Franciscan assemblage, and plotted as a function of distance normal to the San Andreas fault (revised from Borcherdt et al., 1975). The dashed line shows the fit to these intensity estimates obtained by Borcherdt et al. (1975). The solid line shows the intensities for the 1906 earthquake determined by Evernden (1991) for rock-types with the same amplification as Franciscan sandstone. San Francisco intensities A-E were assigned the values 4-0 in Borcherdt et al. (1975).

The Joyner and Boore (1981) model is the seismic source model most widely accepted and understood by engineers. The scaling with seismic moment for each measure of ground motion is obtained empirically. Their model is essentially a point source, but they incorporate the extent of the earthquake by using the closest distance to the surface projection of the rupture area as the measure of source-receiver distance. They assume that all the faults are buried at a single depth, $h = 7.0$ km, estimated by regressing the entire data set. Because the source is not distributed over a set of subsources, as in Evernden's (1991) model, the ground motions predicted near the fault trace are moderate to strong. There is no explicit directivity in their model.

General Model Approach

The modeling approach used in this research has three parts. First, we derive an analytical model that incorporates the three aspects of the earthquake source (scaling, finiteness, and directivity) described in the introduction to estimate the ground motion parameter of the average acceleration spectral level. This parameter has units of velocity rather than acceleration and resembles peak velocity more than peak acceleration. The model is described in the next two sections.

Second, we calibrate this model by fitting the attenuation curve determined by Borcherdt et al. (1975) for the 1906 earthquake. This fitting anchors the relationship between the average acceleration spectral level and intensity. As a second constraint, we consider the variation of intensity with amplification determined by Borcherdt et al. (1975). Our analytical model provides a satisfactory fit to both of these relationships.

Finally, the resulting intensity model was tested for both the 1989 Loma Prieta and the 1984 Morgan Hill earthquake. This second testing process was complicated by the model output (in acceleration power spectral level) being calibrated using the San Francisco intensity scale, which is no longer commonly used. Fitting the observed damage for the 1989 Loma Prieta earthquake is critical, because this earthquake is an analog to most of the scenario events mapped in this report. It also exhibited significant directivity that can be used to statistically constrain the amount of directivity that we then incorporate into the scenario earthquakes. Fitting the damage for the 1984 Morgan Hill earthquake tests the source scaling characteristics of the model. ***Those readers who are not interested in the mathematical derivation of the model may be interested in this section on "Testing..." beginning on page 46.***

A Composite Source Model

The critical components of the composite source model are the subevents, or areal fault elements, distributed at depth below the fault trace. These subevents can be distributed either in a line along strike, at a single depth, or over the area of the rupture surface. Clearly, the linear source model is computationally simpler, and it is reasonable to consider whether an areal source is required to model the relatively large strike-slip earthquakes anticipated for the Bay Area. A sufficiently general source model should be able to accommodate either description, however.

The subevents have two important characteristics. First, they radiate seismic energy (or acceleration spectral amplitude) in azimuthal patterns that exhibit directivity, or a range of possible directivities. Incorporating directivity constitutes the clearest break with the source models used for previous hazard maps. However, we feel that directivity is an important characteristic of almost every intensity pattern observed for large strike-slip earthquakes.

The directivity functions of the subevents should be derived from the rupture process of the earthquake being modeled. If we know the rupture geometry, that is, the rupture direction, ϕ_i, for a subevent or areal element of the fault, we can use the directivity function of Ben-Menahem (1961),

$$D(\phi_i) = \frac{1}{1 - \frac{v}{\beta}\cos\gamma_i}$$

Equation 1

where v is the rupture velocity, β is the shear wave velocity, and γ_i is the angle between the takeoff direction of the shear wave from the i th subevent and the rupture direction ϕ_i as shown in Figure 2.

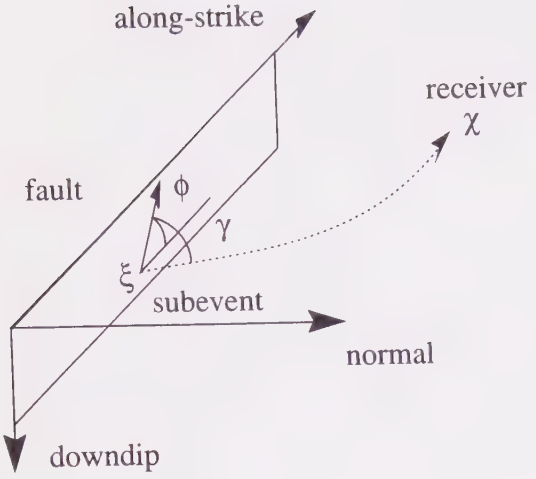

FIGURE 2. A schematic diagram of the relevant angles necessary for the analysis of directivity. The rupture direction is assumed to be partly along strike and partly updip. The angle ϕ is the angle between the rupture direction and the along strike direction. The angle γ is the angle between the rupture direction and the takeoff angle of the wave observed at x.

If we do not know the rupture geometry, but can estimate the probability $P(\phi_i)$ of the rupture direction at i, then we should use the expected directivity D_i, as

$$(D_i)^{\lambda} = \int \frac{P(\phi_i)\,d\phi}{(1-\frac{v}{\beta}\cos\gamma_i)^{\lambda}}$$

Equation 2

in the place of the directivity function. The exponent λ is determined by the coherence of the motions being summed, according to the summation convention discussed below.

The second characteristic of the subevents is that the acceleration power spectrum radiated by a subevent is proportional to $\Delta\sigma^2\Sigma$, where $\Delta\sigma$ is the dynamic stress drop and Σ is the fault area of the subevent. Boatwright (1982) derives the following relationship for the average acceleration spectral level radiated from the ith subevent at ξ to a receiver at x :

$$\left|\ddot{u}_i(x)\right| \propto \frac{D_i\ \Delta\sigma\ \Sigma^{1/2}}{r(\xi, x)}$$

Equation 3

where the geometrical attenuation term $r(\xi,x)$ is assumed to be adequately approximated by the distance between the subevent and the receiver. The average acceleration spectral level is modelled as an average of the Fourier amplitude spectrum of the ground acceleration for frequencies above the corner frequency of the earthquake (Boatwright, 1982). Equation 3 is appropriate for the frequencies of ground motion that can damage most small to moderate-sized structures (0.3 to 3 Hz) for **M**=7 earthquakes, but may overestimate the average acceleration spectral level for **M**<6.5 earthquakes in the direction of rupture. Housner (1970) shows that the undamped velocity response spectrum approximates the Fourier spectrum of the ground acceleration. We note that the average acceleration spectral level has units of velocity rather than acceleration; it scales like peak ground velocity rather than peak ground acceleration.

An important element of the model is the method by which the subevent radiation is summed to estimate the earthquake ground motion. If the wave forms radiated by the subevents were one-sided pulses that shared the same polarity, the subevent radiation would sum coherently as

$$\left|\ddot{u}\right| = \sum_i \left|\ddot{u}_i\right|$$

Equation 4a

commensurate with the exponent $\lambda = 1$. This method of summation is only appropriate for the lowest frequencies radiated by an earthquake, however. The acceleration radiated by the subevents has pulses with both positive and negative polarities that integrate together to zero. That is, the ground stops moving after an earthquake or the subevent of an earthquake. Under this condition, the radiation should be summed incoherently as

$$\left|\ddot{u}\right|^2 = \sum_i \left|\ddot{u}_i\right|^2$$

Equation 4b

commensurate with the exponent $\lambda = 2$ in the directivity function in equation 2. Evernden (1981) uses the exponent $\lambda = 4$ in his summations.

The incoherent summation $\lambda = 2$ was first motivated by Boatwright (1982) to calculate the far-field acceleration from dynamic ruptures. This method of summation is also commensurate with the assumption of a stochastic or random distribution of source strength. The slip and stress drop distributions of large earthquakes appear strongly heterogeneous, rather than uniform. In general, however, we have little knowledge of the spatial variation of the stress drop on a fault surface. For the fault models used in this report, we assume that the stress drop is constant, or uniform, over the rupture area. The source heterogeneity is more readily incorporated using the incoherent sum in equation 4 than by summing over different realizations of a heterogeneous rupture process.

By using an integral over the fault instead of a summation over subevents, the average acceleration spectral level can be written as proportional to the integral

$$|\ddot{u}|^2 \propto \Xi^2 = \int \frac{D^2 \, \Delta\sigma^2}{r^2} d\Sigma$$

Equation 5

where $d\Sigma$ is the incremental fault area and $\Delta\sigma = 1$. To reduce the composite source model to its constituent aspects, it is useful to define integral or fault-average estimates for D and r (retaining the spatially variable stress drop for completeness). These averages are the rms quantities:

$$\left\langle \frac{1}{r} \right\rangle^2 = \frac{1}{\int \Delta\sigma^2 d\Sigma} \int \frac{\Delta\sigma^2}{r^2} d\Sigma$$

$$\langle D \rangle^2 = \frac{1}{\int \frac{\Delta\sigma^2}{r^2} d\Sigma} \int \frac{D^2 \Delta\sigma^2}{r^2} d\Sigma$$

Equations 6 and 7

Manipulating equation 5 by algebraic substitution and taking the square root of both sides, we obtain the simple form:

$$\Xi = \left\langle \frac{1}{r} \right\rangle \langle D \rangle \left[\int \Delta\sigma^2 d\Sigma \right]^{1/2}$$

Equation 8

This form makes explicit the three aspects of the seismic source discussed in the Introduction. The term $\langle 1/r \rangle$ contains the source finiteness effect, explicitly calculated as the root mean square inverse distance from the fault surface. This term depends only on the spatial extent of the source and the distribution of stress drop. The second term $\langle D \rangle$ contains the effect of directivity or focusing, possibly obtained from an expectation over a set of rupture geometries. The last term $\left[\int \Delta\sigma^2 d\Sigma \right]^{1/2}$ contains a measure of the overall source strength that is independent of the source-receiver geometry and rupture geometry. This last term is the source scaling term.

A Trilateral Rupture Model

In general, the problem of determining the directivity is relatively difficult, requiring an expectation over the set of possible rupture geometries for the fault segment. For large strike-slip faults, however, the predominate directions of rupture propagation are horizontal and updip. The rupture propagates horizontally along strike, either unilaterally or bilaterally, and it propagates updip because of the general increase of seismic velocity with depth; effectively, the faster rupture of the deeper areas of the fault drives the rupture of the shallower fault areas. In addition, the general increase of the stress state with depth implies that ruptures usually start at depth and rupture updip (Das and Scholz, 1983). Figure 3 shows a schematic of the rupture growth on such a fault; the rupture propagates horizontally on the deeper sections and vertically on the shallower sections of the fault.

For such a fault, we approximate the probability for the direction of rupture at each subevent as $P(\phi = 0°, 90°, 180°) = 1/3$. The resulting directivity function is

$$D_i^2 = \frac{1}{3(1-\frac{v}{\beta}\cos\gamma_+)^2} + \frac{1}{3(1-\frac{v}{\beta}\cos\gamma_-)^2} + \frac{1}{3(1-\frac{\upsilon}{\beta}\cos\eta)^2}$$

Equation 9

where v is the horizontal rupture velocity, $\gamma_+ = \pi - \gamma_-$ are the appropriate direction cosines for horizontal rupture in the two directions along strike, υ is the updip rupture velocity, and η is the direction cosine for updip rupture.

For simplicity, all subevents on the fault are assumed to share this same directivity function. Although computationally simple, the trilateral rupture yields an adequate approximation of the expectation over the three most obvious rupture geometries (unilateral, starting at either end of the fault, and bilateral).

To calculate the acceleration spectral level, then, we numerically integrate equation 5 over a line of subsources at the fixed depth of 5 km, between the specified ends of the rupture. The stress drop is assumed to be constant at $\Delta\sigma = 1$, and the trilateral directivity function in equation 9 is used for each subsource. Using a line source to model these large strike-slip faults reduces the integrand $d\Sigma = w d\ell$ where w is the total width of the fault, and $d\ell$ is the incremental length evaluated in the numerical integration. Note that this integration does not require specifiying the time dependence of the rupture process, only its incoherence. The square root of the resulting integral yields the (normalized) estimate of the average acceleration spectral level.

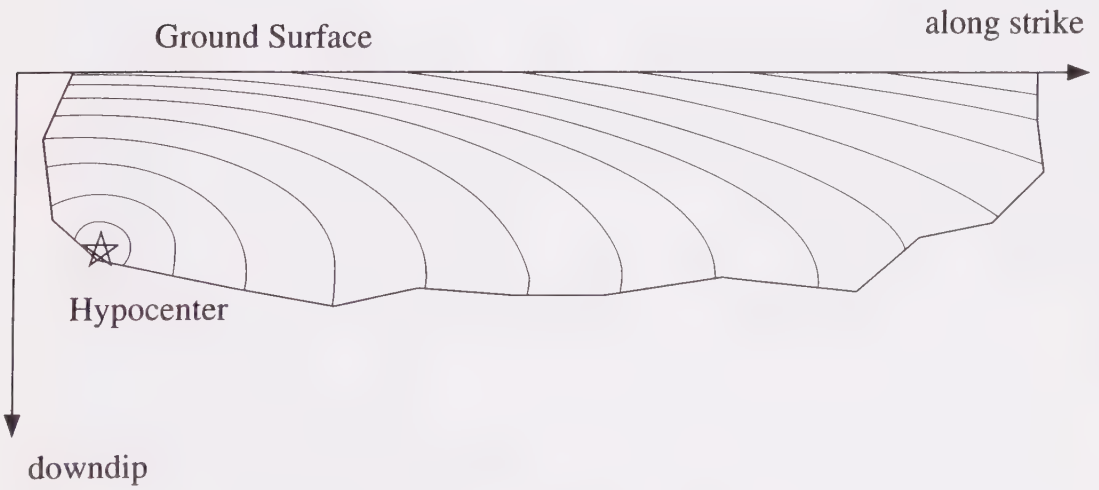

FIGURE 3. A schematic diagram of rupture propagation (plotted as rupture fronts at equal time increments) on a long strike-slip fault embedded in a crustal velocity structure in which the S-wave velocity increases with depth. The faster horizontal rupture of the deepest segment of the fault drives the updip rupture process on the shallower segments.

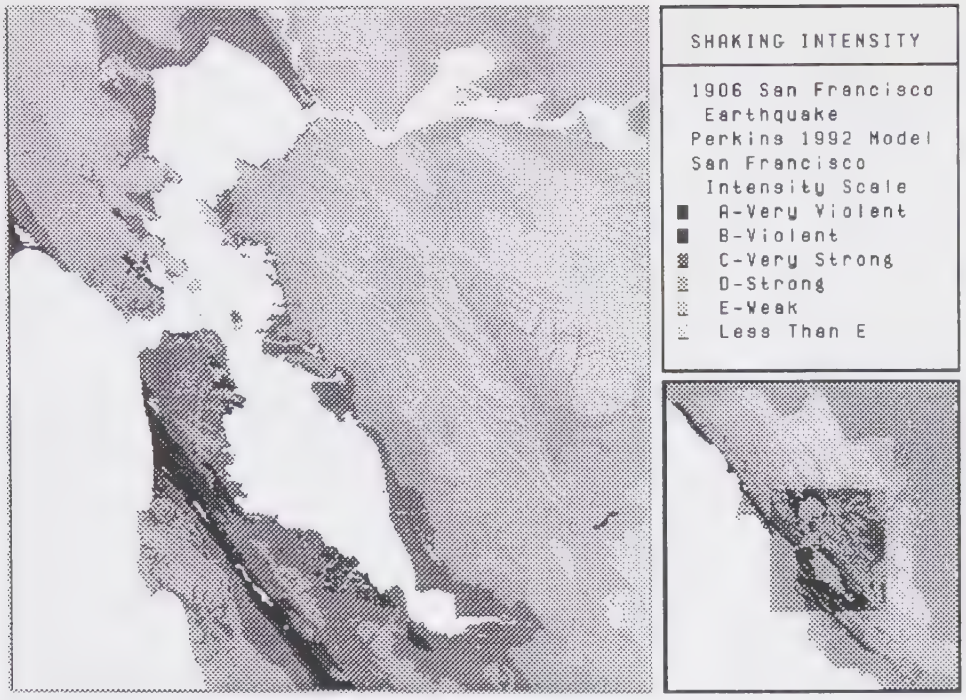

PLATE 1a -- Map showing intensities for a repeat of the 1906 San Francisco earthquake based on the attenuation relationship described in Borcherdt et al. (1975) and used as a model in Perkins (1992) with the intensity increments described in Appendix B.

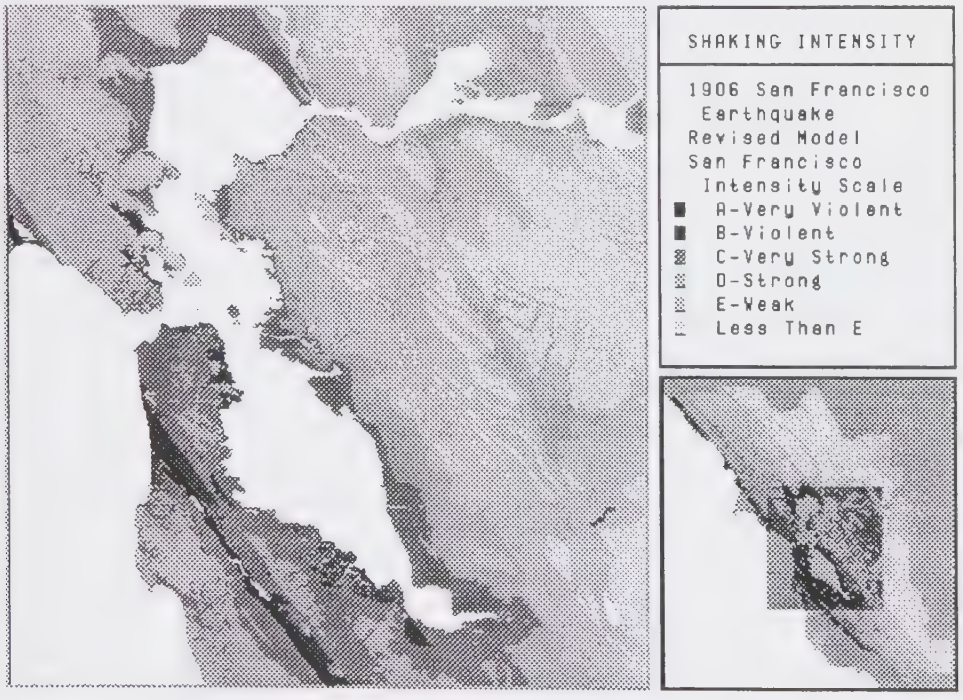

PLATE 1b -- Map showing intensities for a repeat of the 1906 San Francisco earthquake based on the revised relationships described in this Appendix, with the intensity increments described in Appendix B.

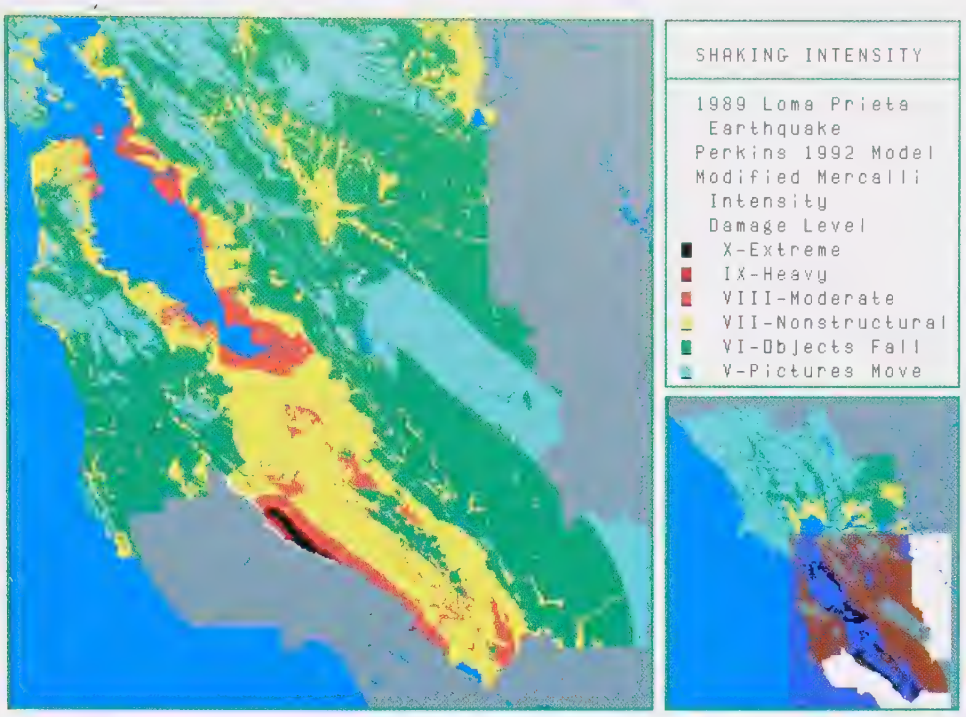

PLATE 2a -- Map showing intensities for a repeat of the 1989 Loma Prieta earthquake based on the model described in Borcherdt et al. (1975) and used as a model in Perkins (1992), with the intensity increments described in Appendix B.

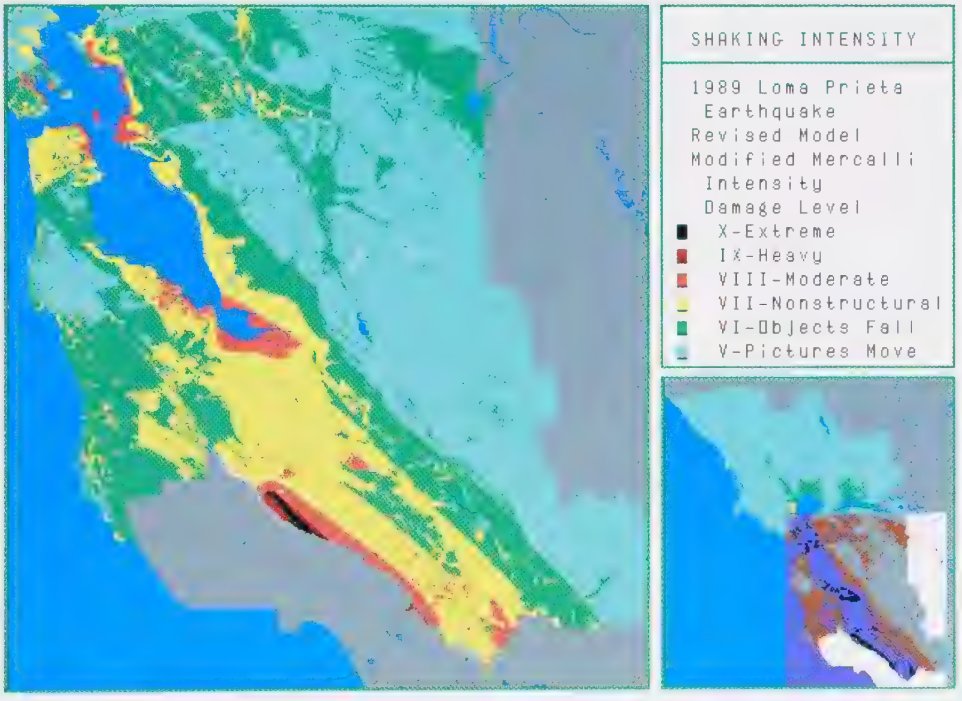

PLATE 2b -- Map showing intensities for a repeat of the 1989 Loma Prieta earthquake based on the revised relationships described in this Appendix, with the intensity increments described in Appendix B.

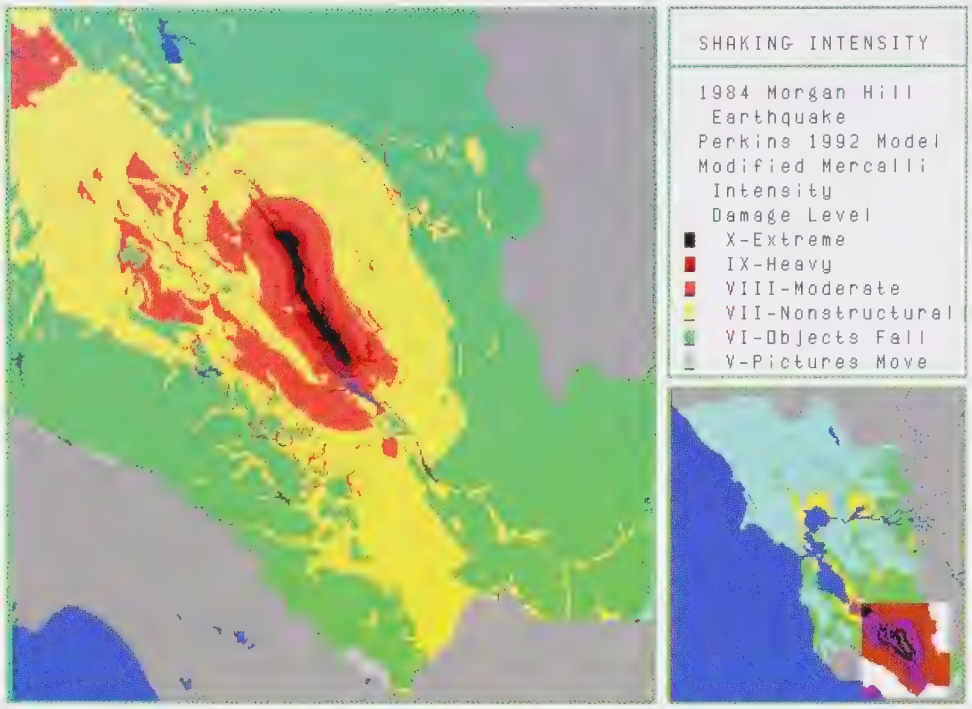

PLATE 3a -- Map showing intensities for a repeat of the 1984 Morgan Hill earthquake based on the model described in Borcherdt et al. (1975) and used as a model in Perkins (1992), with the intensity increments described in Appendix B.

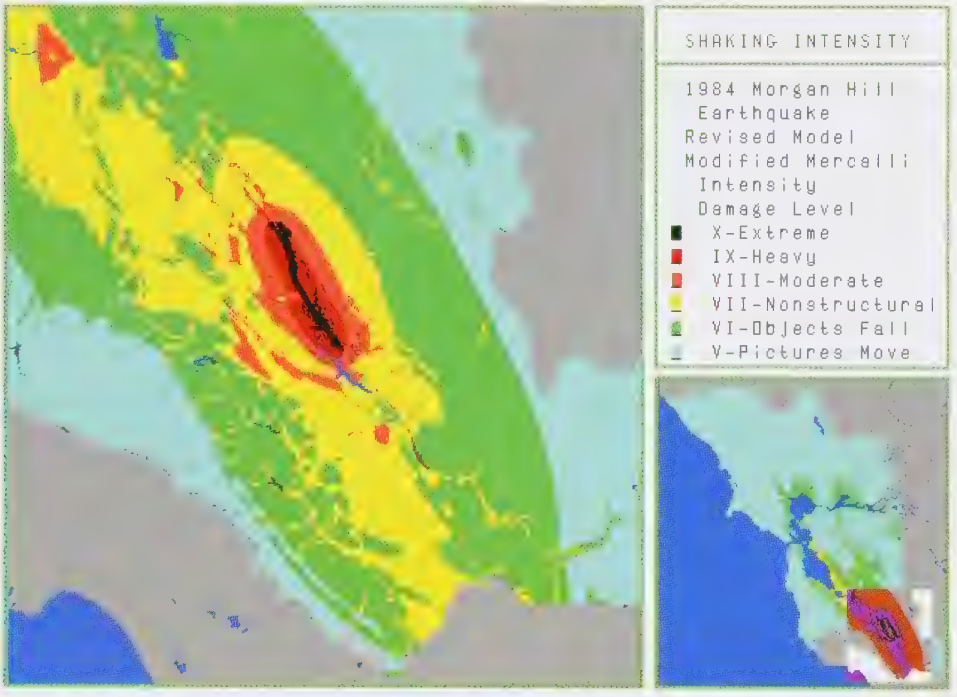

PLATE 3b -- Map showing intensities for a repeat of the 1984 Morgan Hill earthquake based on the revised relationships described in this Appendix, with the intensity increments described in Appendix B.

Calibrating Intensities Normal to the Fault Trace

Before we can apply this model to the problem of predicting intensities, however, we need to calibrate the relationship between intensity and ground motion for large strike-slip faults. We obtain this calibration by fitting the logarithm of the predicted acceleration spectral level for a 400-km-long fault to the intensities plotted in Figure 1 by Borcherdt et al. (1975).

Using the rupture velocities $v = 0.8\beta$ and $\upsilon = 0.95\beta$ in the model, we can fit the level and falloff of the 1906 intensities normal to this fault using the relation,

$$I_{1906} = 1.0 + 3.0 \log(\Xi)$$

Equation 10

The fit is plotted in Figure 4. This comparison makes the motivation for using different velocities for the horizontal and vertical rupture processes clear. The ground motions near the trace of the fault are dominated by the updip directivity, that is, the third term in equation 8. It is necessary to use an artificially fast updip rupture velocity to fit the strong intensities observed near the fault in the 1906 earthquake. Even with this high a rupture velocity, the intensities observed closest to the fault are somewhat underestimated by this model. Borcherdt et al. (1975) fit the intensity data as a function of distance both using and not using the data in the immediate fault zone and obtained essentially the same attenuation relationship.

It is possible that the high intensities observed within 2 km of the fault are the result of the low-velocity zone associated with the fault itself. These narrow low-velocity zones act as wave guides for shear waves with periods from 0.3 to 1 s (see Li et al., 1994). The major strike-slip faults in the Bay Area have pronounced low-velocity zones whose widths range from 100 m to 2 km. These low-velocity zones channel and strongly amplify transversely polarized shear waves, the strongest waves radiated by a strike-slip earthquake. A more sophisticated model for the ground motions would incorporate this amplification through a factor that depends on the distance from the fault trace; the updip rupture velocity required to fit such a model to the observed intensities could be as low as $v = 0.8\beta$, depending on the assumed near-fault amplification factor.

In order to fit the intensities expected near the fault trace, all areas within 0.2 km of the surface expression of the fault have been assigned the highest intensity. From a practical standpoint, the remaining areas where the revised model underestimates the 1906 intensities are not significant unless the area has an intensity increment less than 0.5 (in effect, soft rock). Larger intensity increments raise the estimated intensity above $I_{1906} = 3.0$. See Plates 1a and 1b.

We note the similarity between equation 10 and the relationship determined by Borcherdt et al. (1975)

$$\delta I = 0.19 + 2.97 \log(AHSA)$$

Equation 11

for the intensity increment δI associated with the average horizontal spectral amplification *AHSA* obtained from all the recording sites in the Bay Area at which there were intensity estimates for the 1906 earthquake. The coefficient of 3.0 in equation 10 is essentially the same as the coefficient 2.97. Since the average acceleration spectral level Ξ is modified linearly by the average horizontal spectral amplification, that is, $I + \delta I \propto 3.0 \log(AHSA * \Xi)$, the coincidence of these two coefficients indicates that the fit obtained in Figure 4 is not fortuitous, and that intensity is proportional to the logarithm of the cube of the ground motion.

Finally, it is possible to quantify the proportionality in equation 5 and estimate the average acceleration spectral level, or equivalently, the undamped velocity response spectrum. By combining equation 5 with equation 15 in Boatwright (1982), taking averages of the various components of the high-frequency radiation pattern in equation 2 of Boatwright (1982), and assuming ρ = 2.7 gm/cm^3, β = 3.5 km/s at depth, Δv = 0.8, β = 2.8 km/s, $\Delta\sigma$ = 50 bars, ρ = 2.0 gm/cm^3 and β = 0.8 km/s for Franciscan sandstone, we obtain the simple relation

$$|\ddot{u}| \cong 20\Xi \text{ cm/s} \qquad \textit{Equation 12}$$

where Ξ is calculated in equation 5 with $\Delta\sigma = 1$. Combining this relation with equation 10 gives estimates of the average acceleration spectral level, or equivalently, the undamped velocity response spectrum, associated with the MMI and 1906 intensity levels, as shown in Table 1.

TABLE 1. Approximate Relationships Among Intensity Scales and Average Acceleration Spectral Level
NOTE - Average acceleration spectral level is equivalent, but not identical, to undamped velocity response spectra, as discussed in the text. It has units of velocity, not acceleration.

Modified Mercalli Intensity	San Francisco Intensity	Average Acceleration Spectral Level
XII - Massive Destruction		(MMI XII - not shaking related)
XI - Utilities Destroyed	A - Very Violent	
X - Most Small Structures Destroyed		150 cm/sec
	B - Violent	100 cm/sec
IX - Heavy Damage		68 cm/sec
	C - Very Strong	47 cm/sec
VIII - Moderate to Heavy Damage		32 cm/sec
	D - Strong	22 cm/sec
VII - General Nonstructural Damage		15 cm/sec
	E - Weak	10 cm/sec
VI - Felt by All, Books Off Shelves		7 cm/sec
	< E - Very Weak	5 cm/sec
V - Wakes Sleepers, Pictures Move		3 cm/sec

Testing the Intensity Model by Comparing Actual Versus Predicted Red-Tagged Housing Units in Past Bay Area Earthquakes

The key test for any mapping scheme which proposes to predict the intensity patterns of future earthquakes is its ability to accurately "model" intensity patterns in past earthquakes. In the case of these maps, the principal comparison was made not with the modified Mercalli intensity map published for the Loma Prieta earthquake (Stover et al., 1990), but with actual housing damage patterns from that earthquake as measured by red-tagged dwelling units of various construction types. These units are in buildings which were "red-tagged" as being unsafe to occupy using a set of criteria published by the California Office of Emergency Services and used fairly uniformly by all of the city and county building inspection departments.

The testing process involved a comparison of predicted red-tagged units to actual red-tagged units. First, alternative models to predict intensity patterns in the Loma Prieta earthquake were generated using either the attenuation relationship of Borcherdt et al. (1975) without magnitude scaling or directivity, or the model based on the average acceleration spectral level. A second model was then run for each resulting intensity map to predict the number of red-tagged units. This second model uses estimates of the existing land use, the housing stock, and the damage matrices that relate the percent of red-tagged units by construction type to the intensity. These predictions are then systematically compared with the actual red-tagged unit counts for that earthquake for twelve building types, for each of the cities and counties in the region. The error analysis consisted of calculating the mean absolute error (MAE) and root mean square error (RMSE) for the county/ building type and community data. These error measurements were used rather than the percentage error due to the large number of zero values in the data when no actual red-tagged units were present.

This testing process was a reiterative exercise; actual red-tagged units were compared with revised predictions for the number of those units based on increasingly sophisticated assumptions about the role of directivity and the additional complication of the propagation effect associated with the Mohorovicic discontinuity (the boundary between the crust and the mantle), as well as on improved data on existing land use and building construction/unit counts for the time of the Loma Prieta earthquake. A total of over seventy models were run for this earthquake.

The two models with the "best" fit were used to create a revised matrix relating intensity percent red-tagged by modified Mercalli intensity by construction type based on the actual damage data from the Loma Prieta earthquake to predict red-tagged units. This "modified" matrix was then used to estimate the red-tagged units again, reducing the errors even further. However, the changes in the

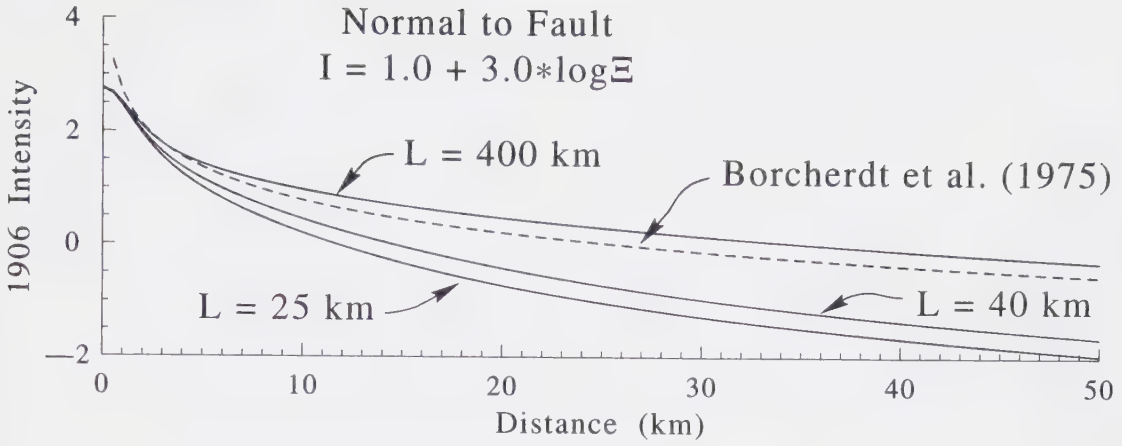

FIGURE 4. The attenuation normal to the fault for three different rupture lengths (L = 200, 40, and 25 km). These rupture lengths correspond roughly to the 1906 San Francisco earthquake, the 1989 Loma Prieta earthquake, and the 1984 Morgan Hill earthquake. The dashed line shows the fit obtained by Borcherdt et al. (1975) to the 1906 intensities. The smaller the fault length, the more rapidly the intensity attenuates away from the fault.

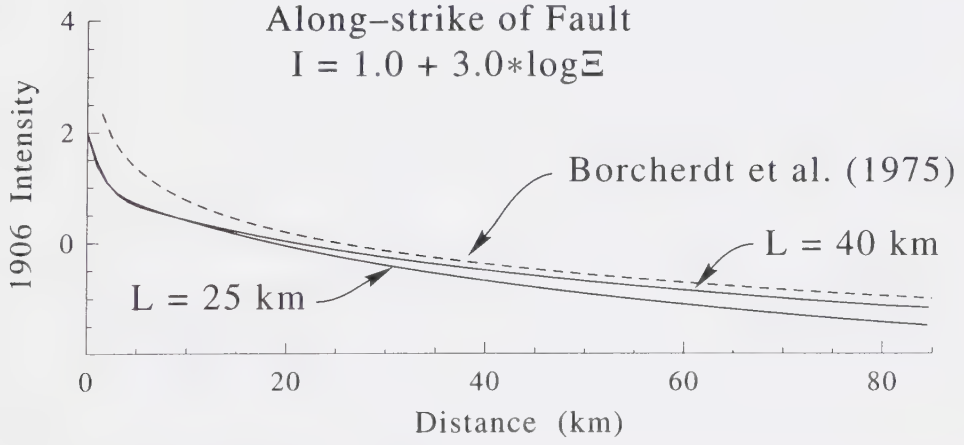

FIGURE 5. The attenuation along the fault for two different rupture lengths (L = 40 and 25 km). The dashed line shows the fit obtained by Borcherdt et al. (1975) to the 1906 intensities normal to the San Andreas fault. The attenuation of intensity as a function of distance along strike of the fault does not depend strongly on the fault length.

matrix were conservative, reflecting our respect for the quality of the data from earlier earthquakes that went into the original matrix.

The baseline error analysis using the revised damage matrix run for the "original" model (from Perkins, 1992, based on the closest point to the surface expression of the fault and the attenuation relationship of Borcherdt et al., 1975), yielded a MAE of 34.88 units by city area. This model overestimated the red-tagged units in Santa Clara County by one-third and underestimated the red-tagged units in San Francisco by a factor of twelve. The MAE was increased when a Moho "bounce" of one intensity unit was added for distances above 50 km from the end of the fault (to 37.01), but decreased (to 29.52) when a bounce of one-half an intensity unit was used.

The best fit was obtained by using the trilateral directivity model for the average acceleration spectral level in equation 5 and a Moho bounce for distances from 70 to 90 km from the end of the fault. Using $v = 0.8\beta$ as the horizontal rupture velocity and a Moho bounce of one intensity unit yields approximately the same MAE (27.80 units by city area) as $v = 0.85\beta$ and a Moho bounce of half an intensity unit (27.58). Although the damage data from Santa Cruz and San Benito Counties were not included in this analysis, the cities of Watsonville and Hollister, which lie along the fault strike to the southeast, also had higher than expected damage.

In addition, because the source model used for this mapping incorporates updip directivity, it agrees with the strong evidence for increased damage near the (unruptured) fault trace. The near-fault area exposed to modified Mercalli intensities IX and X is dominated by single family homes built prior to 1940. Over one-third of these homes were red-tagged, while only 2% of similar homes exposed to MMI VIII were red-tagged. Both the original model of Perkins (1992), based on the attenuation relationship of Borcherdt at al. (1975), and the model derived in this Appendix fit this near-fault damage.

An improvement of the model derived in this Appendix is the simultaneous decrease of the predicted number of wood-frame dwellings and mobile homes damaged in Santa Clara County and increase of the predicted number of damaged units in Oakland and San Francisco. The original model of Perkins (1992) based on the attenuation relationship of Borcherdt et al. (1975) overpredicts the damage in Santa Clara County. See Plates 2a and 2b for a comparison of the outputs of these two models.

The directivity model was then tested for a much smaller earthquake, the Morgan Hill earthquake of 1984. This $\boldsymbol{M} = 6.4$ earthquake is at the lower end of the magnitude scale of the scenario earthquakes to be modeled. The trilateral-rupture model predicted a total of 202 red-tagged units, larger than the 39 units that were actually red-tagged, but much smaller than the 1089 red-tagged units predicted by the original model. For this fit, we used a trilateral-rupture model with $v = 0.8\beta$. The Morgan Hill earthquake ruptured predominately from northwest to southeast (Beroza and Spudich, 1988). A source model with more directivity to the southeast than the northwest would yield a better fit to the number of red-tagged units. See Plates 3a and 3b for a comparison of the output of the two models.

Another recent moderate earthquake was the 1980 Livermore earthquake. The role of directivitiy in this earthquake has previously been examined by Boatwright and Boore (1982).

Conclusion

The exercise of fitting the damage associated with the 1906 San Francisco earthquake, the 1989 Loma Prieta earthquake and the 1984 Morgan Hill earthquake clearly indicates that the intensity models developed in the mid-1970s that ABAG has been using, with minor modifications, for almost twenty years have been improved by including directivity. In particular, the fit to the 1989 Loma Prieta damage provides a critical test of these intensity models, improving our ability to predict intensities for areas lying along strike from these large scenario earthquakes.

An additional improvement is the magnitude scaling derived from the physical model of the source. This scaling allows intensities to remain high near the fault, while falling off more abruptly perpendicular to the fault as the magnitude decreases. The steepness of this fall-off is less pronounced along the fault strike. These effects are significant for the range of magnitudes associated with expected future damaging earthquakes in the Bay Area.

TECHNICAL APPENDIX B -- OCCURRENCE OF AND AVERAGE PREDICTED INTENSITY INCREMENTS FOR THE GEOLOGIC UNITS IN THE SAN FRANCISCO BAY AREA

The average predicted intensity increments for the geologic units in the San Francisco Bay Area are based on the properties of the materials contained in those units. The predicted intensity increments from Table B1 are averaged for each geologic unit listed in Table B3 based on those materials.

These intensity increments (δI or fractional changes in intensity) are added to (or subtracted from) intensities calculated from the distance/directivity relationship described in Appendix A to generate the intensity map.

TABLE B1– SEISMICALLY DISTINCT UNITS AND PREDICTED INTENSITY INCREMENTS

[modified from Borcherdt, Gibbs and Fumal (1978) based on additional shear wave velocity (v) measurements in Borcherdt and Glassmoyer (1992) and the amplification formula in Borcherdt (1994) of $F_v = (1050\ m/s/v)^{0.65}$. Then the formula $\delta I = 0.19 + 2.97 \log (F_v)$ from Borcherdt et al. (1975) was used to convert amplification to intensity increments.]

Seismic Unit for Sediments	Material Properties	Predicted Intensity Increment
I	Clay and silty clay, very soft to soft	2.4
II	Clay and silty clay, medium to hard	1.8
III	Sand, loose to dense	1.6
IV	Sandy clay-silt loam, interbedded coarse and fine sediment	1.4
V	Sand, dense to very dense	1.1
VI	Gravel	0.7

Seismic Unit for Bedrock	Rock Type	Hardness	Fracture Spacing	Predicted Intensity Increment
I	Sandstone	Firm to soft	Moderate and wider	1.0
II	Igneous rocks, Sedimentary rocks	Hard to soft	Close to very close	0.7
III	Igneous rocks, Sandstone, Shale	Hard to firm	Close	0.5
IV	Igneous rocks, Sandstone	Hard to firm	Close to moderate	0.3
V	Sandstone, Conglomerate	Firm to hard	Moderate and wider	0.2
VI	Sandstone	Hard to quite firm	Moderate and wider	0
VII	Igneous rocks	Hard	Close to moderate	-0.2

TABLE B2 – SOURCE MAP REFERENCES BY AREA

Area	Author	Source Map Scale
All Flatlands Areas (except in San Mateo County)	Burke, Helley, and others, 1979	1:125,000
Northwest Area	Blake, Smith, and others, 1971	1:62,500
North Central Area	Fox, Sims, and others, 1973	1:62,500
Northeast Area	Sims, Fox, and others, 1973	1:62,500
Central Marin Area	Blake, Bartow, and others, 1974	1:62,500
Central East Area	Brabb, Sonneman, and others, 1971	1:62,500
East Bay Area	Dibblee, 1972 to 1981	1:24,500
Southeast Area	Cotton, 1972	1:62,500
Southwest Santa Clara Area	Brabb and Dibblee, 1978 to 1980	1:24,500
Northwest Santa Clara Area	Brabb, 1970	1:62,500
San Mateo Area	Brabb and Pampeyan, 1983	1:62,500
South San Francisco Area	Bonilla, 1971	1:24,000
North San Francisco Area	Schlocker, Bonilla and Radbruch, 1958	1:24,000
West Alameda Area	Brabb, unpublished	1:62,500
Oakland Area	Radbruch, 1957 and 1969	1:24,000

FIGURE – SOURCE MAP AREAS FOR GEOLOGIC INFORMATION

(using a USGS 7.5' quadrangle index map as a base map)

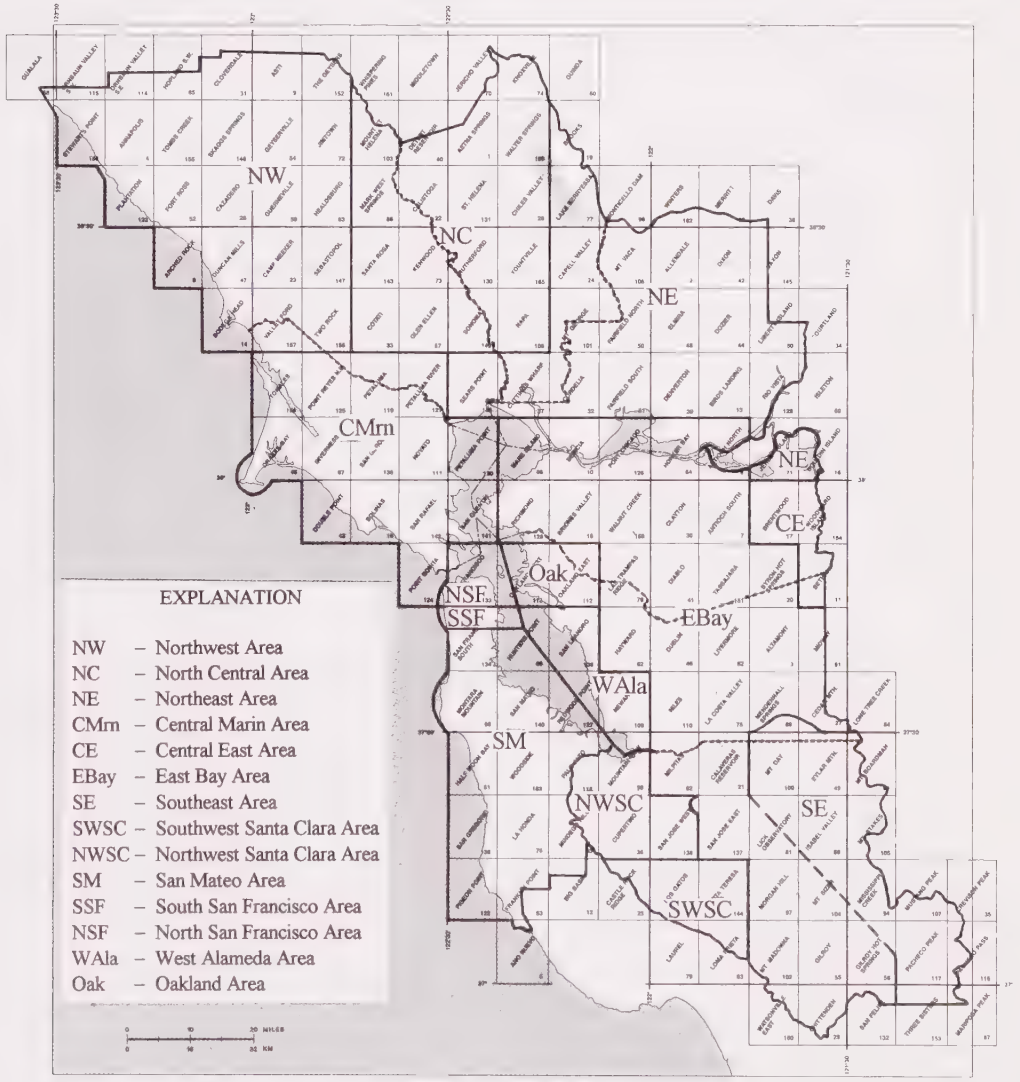

TABLE B3 -- OCCURRENCE OF AND AVERAGE PREDICTED INTENSITY INCREMENTS FOR THE GEOLOGIC UNITS IN THE SAN FRANCISCO BAY AREA

[Seismic units present are modified and expanded from Fumal (1978) based on pers. comm. with T. Fumal and J. Gibbs (1978 to 1983) and data on Merritt sand in Borcherdt and Glassmoyer (1992). The strategraphic nomenclature and unit age assignments used in this table may not necessarily conform to current usage by the U.S. Geological Survey.]

Map Symbol (s)	Geologic Unit	Source Map	Seismic Units Present	Average Predicted Intensity Increment
Quaternary Units				
1. Qu	Undivided Quaternary alluvium (due to occurrence in urban areas)	Flat	II, III, IV, V, VI	1.3
2. Qhaf (purple); Qaf	Artificial fill	Flat; CE; SM	II, III, V	1.5
3. Qhsc; Qal	Holocene stream channel deposits	Flat; SM	III, V	1.4
4. Qhac; Qyf	Holocene coarse-grained alluvium; fan and basin deposits	Flat; SM	V	1.1
5. Qham; Qyfo	Holocene medium-grained alluvium; fan and plain deposits	Flat; SM	III	1.6
6. Qhaf; Qb	Holocene fine-grained alluvium; fan and plain (basin) deposits	Flat; SM	II	1.8
7. Qhafs	Holocene fine-grained alluvium; fan and plain (basin) deposits–salt-affected	Flat	II	1.8
8. Qhbm; Qm	Holocene Bay mud	Flat; SM	I	2.4
9. Qcl	Holocene colluvium; slope wash and ravine fill	SM; data gaps	III, V	1.4
10. Qhs; Qs	Holocene beach and windblown sand	Flat; SM	III, V	1.4
11. Qpa	Pleistocene alluvium	Flat	V, VI	0.9
12. Qps	Pleistocene sand; Merritt sand	Flat	II	1.8
13. Qpea	Early Pleistocene alluvium	Flat	V, VI	0.9
14. Qof	Pleistocene coarse-grained alluvium; fan deposits	SM	V, VI	0.9
15. Qob	Pleistocene fine-grained alluvium; basin deposits	SM	II, IV	1.6
16. Qpmt; Qmt	Pleistocene marine terrace deposits	Flat; SM	V	1.1
17. Qm	Quaternary Montezuma Formation	NE	V	1.1
18. Qr	Quaternary tuff and gravel from rhyolite	NC; NE, CMm	V, VI	0.9
19. Qg	Quaternary gravel, poorly bedded	NC	V, VI	0.9
20. Qg	Quaternary stream gravel and sand	EBay; SWSC	III, V	1.4
21. Qr	Quaternary rhyolite of the Clear Lake area	NW; adj. area on NC	III, VII	0.2
22. Qclt	Quaternary Clear Lake area tuff	NW; NC	I, II	0.8
23. Qob	Quaternary olivine basalt of Clear Lake area	NC	II, VII	0.2
24. Qmi	Quaternary Millerton Formation	CMm	III, VI	1.2
25. Qpmc; Qc	Quaternary Colma Formation	Flat; CMm; SSF; NSF	V	1.1
26. Qlv	Quaternary boulder gravels of volcanic debris	EBay	VI	0.7
Quaternary/Tertiary Units				
27. QTs; Qsc	Santa Clara Formation	EBay; SWSC; SM; NWSC	III, IV, V, VI, V, VII	0.8
28. Qsb	Santa Clara Formation–gravel with basalt detritus	EBay	V, VI	0.9
29. Qsp	Santa Clara Formation–conglomerate or breccia detritus	EBay	VI	0.7
30. Qsa	Santa Clara Formation–clay	EBay	III	1.6
31. Qsc w/a	Santa Clara Formation–andesite	EBay	VII	-0.2
32. Qsc w/b	Santa Clara Formation–basalt	EBay	VII	-0.2
33. QThg	Huichica and Glen Ellen Formation	NC; NE	VI, I	0.8
34. QTge	Glen Ellen Formation	NW	VI, I	0.8
35. QTget	Glen Ellen Formation with tuff	NW	VI, I	0.8
36. QTc	Cache Formation	NC	I	1.0
37. QTl	Livermore Gravel	EBay	III, IV, V, VI	1.2
38. QTt	Tassajara Formation	EBay	III, IV, V	1.4
39. QTb	Unnamed olivine basalt lava	EBay	VII	-0.2
40. bi	Intrusive basalt in QTb	EBay	VII	-0.2
41. QTp	Paso Robles Formation	EBay	II, V, VI	1.2
42. Qtm; Tm; Tme (?)	Merced Formation	NW; NC; CMm; SM; SSF; NWSC	I	1.0
Tertiary Units (Pliocene)				
43. Tp	Pliocene Purisima Formation–undivided	EBay; SWSC; SM	I, II	0.8
44. Tptu	Pliocene Tunitas Sandstone Member of the Purisima Fm.	SM	I, II	0.8
45. Tpl	Pliocene Lobitos Mudstone Member of the Purisima Fm.	SM	I	1.0
46. Tpsg	Pliocene San Gregorio Sandstone Member of the Purisima Formation	SM	I, II	0.8
47. Tpp	Pliocene Pomponio Siltstone Member of the Purisima Fm.	SM	II, III	0.6
48. Tpt	Pliocene Tehama Sandstone and Siltstone Member of the Purisima Formation	SM	I, II	0.8
49. Tor	Pliocene Ohlson Ranch Formation	NW	I	1.0
50. Tors	Pliocene Ohlson Ranch Formation–sandstone	NW	I	1.0

Map Symbol (s)	Geologic Unit	Source Map	Seismic Units Present	Average Predicted Intensity Increment
51. Torc	Pliocene Ohlson Ranch Formation--conglomerate	NW	IV	1.4
52. Tpt	Pliocene Tuff of Putah Creek	NE	I, II	0.8
53. Tlt; Tpl	Pliocene Lawlor Tuff	NE	I, II	0.8
54. Tp	Pliocene Petaluma Formation--undivided	NC	I, II	0.8
55. Tps	Pliocene Petaluma Fm.--claystone, siltstone and mudstone	NE; CMm	I, II	0.8
56. Tpc	Pliocene Petaluma Formation--imbedded gray claystone	NE; CMm	I, II	0.8
57. Tp (?)	Pliocene Petaluma Formation--questionable	NW	I, II	0.8
58. Tsv	Pliocene Sonoma Volcanics--undivided	NE; CMm	I, II, III, VII	0.5
59. Tsr	Pliocene Sonoma Volcanics--rhyolitic lava flows	NC; NE; CMm	IV, V, VI, VII	0.1
60. Tsri	Pliocene Sonoma Volcanics--rhyolitic plugs and dikes	NC; NE; CMm	II, III, VII	0.3
61. Tsrs	Pliocene Sonoma Volcanics--soda rhyolite flows	NC	VII	-0.2
62. Tsrp	Pliocene Sonoma Volcanics--perlitic rhyolite	NC; NE	VII	-0.2
63. Tsrb	Pliocene Sonoma Volcanics--rhyolitic breccia	NW; NC	VII	-0.2
64. Tsa	Pliocene Sonoma Volcanics--andesitic to basaltic lava flows	NC; NE; CMm	III, VII	0.2
65. Tsai	Pliocene Sonoma Volcanics--andesitic to dacitic plugs	NC; NE	VII	-0.2
66. Tsfd	Pliocene Sonoma Volcanics--basaltic or andesitic lava flows with diatomite	NC	I, VII	0.4
67. Tsb	Pliocene Sonoma Volcanics--basalt	NW	VII	-0.2
68. Tst	Pliocene Sonoma Volcanics--pumicitic ash-flow tuff	NC; NE; CMm	I, II, VII	0.5
69. Tswt	Pliocene Sonoma Volcanics--welded ash-flow tuff	NC; NE	II, VII	0.2
70. Tstx	Pliocene Sonoma Volcanics--tuff (?), welded, massive, hard, xenolithic	NC	VII	-0.2
71. Tsag	Pliocene Sonoma Volcanics--agglomerate	NC; NE	II, III	0.6
72. Tslt	Pliocene Sonoma Volcanics--tuff breccia	NC; NE	II, III, VI	0.4
73. Tsft	Pliocene Sonoma Volcanics--pumicitic ash-flow tuff with lava flows	NC	I, II, VII	0.5
74. Tss	Pliocene Sonoma Volcanics--sedimentary deposits	NC; NE	VI, I, II	0.8
75. Tssd	Pliocene Sonoma Volcanics--diatomite	NC; NE	I, II, VI	0.6
76. rh	Pliocene rhyolite; includes the Alum Rock Rhyolite and Leona Rhyolite	EBay; Oak; WAla	III, IV, V, VI, VII	0.2
77. Tb; Tbu	Pliocene unnamed basalt; included basalt in the Orinda Fm.	EBay	II, VI	0.4
78. Tri	Pliocene rhyolitic intrusive	EBay	VII	-0.2
79. a	Pliocene andesitic rock	EBay	VII	-0.2
80. Tpb	Pliocene Putnam Peak Basalt	NE	VII	-0.2
81. Tcu	Pliocene Contra Costa Group--undivided	Oak	I, II, IV	0.7
82. Tbp	Pliocene Bald Peak Basalt	EBay; Oak	II, VII	0.2
83. Ts	Pliocene Siesta Formation	Oak	II, III, IV	0.6
84. Tmb	Pliocene Moraga Formation--basalt and andesite	EBay; Oak	VI, VII	-0.1
85. Tmt; Tmc	Pliocene Moraga Fm.--clastic rocks, including tuff breccia	EBay; Oak	II, III	0.6
86. Tps; Tor; Tw; Tpo; Tpth; Tol; Tsc	Pliocene non-marine sedimentary rocks, locally called the Orinda, Wolfskill, Tehama or Oro Loma	NE; CE; EBay; Oak	I, II, III, IV, V	0.5
87. Tpl	Pliocene lacustrine limestone	EBay	VI	0.0
88. Tpt	Pliocene tuff and sandstone, including the Pinole Tuff	EBay	III, VI	0.2
89. Tpc; Tuc	Pliocene non-marine sedimentary rocks, clay with sandstone and conglomerate	EBay	VI, I, II	0.8
90. Tcg	Pliocene non-marine pebble conglomerate	EBay	VI	0.7
91. Tus	Pliocene non-marine sandstone	EBay	II, IV	0.5
92. Te	Pliocene Etchegoin Formation	EBay	I, II	0.8
Tertiary Units (Plicene/Miocene)				
93. Tsc	Pliocene/Miocene Santa Cruz Mudstone	SM	II, III	0.6
94. Tsm	Pliocene/Miocene Santa Margarita Sandstone	SM	I, II	0.8
95. Tvia; Tv	Pliocene/Miocene Quien Sabe Volcanics--intrusive andesitic rocks	EBay; SE	VII	-0.2
96. Tpx	Pliocene/Miocene sandstone--probably a large clastic dike	CMm	VI	0.0
97. Tdbc	Pliocene/Miocene Drakes Bay siltstone and mudstone	CMm	II, III	0.6
98. Tdbs	Pliocene/Miocene Drakes Bay glaucomitic sandstone	CMm	I, II	0.8
Tertiary Units (Miocene)				
99. Tsm	Miocene sandstone and mudstone in Skaggs and Duncans Mills quadrangles	NW	I, II	0.8
100. Tn, Tmn	Miocene Neroly Sandstone	NE; CE; EBay	I, II	0.8
101. Tn (?)	Miocene questionable Neroly Sandstone	NC	I, II	0.8
102. Tmss; Tmb, Tbr; Tmci	Niocene sandstone, including the Cierbo and Briones Formations	NE; EBay	IV, VI	0.2
103. Tmbu	Miocene Briones Sandstone--upper member (sandstone)	NE	IV, V, VI	0.2
104. Tmbm	Miocene Briones Sandstone--middle member (light gray siliceous shale)	NE	II, III	0.6
105. Tmbl	Miocene Briones Sandstone--lower member (sandstone)	NE	IV, V, VI	0.2

Map Symbol (s)	Geologic Unit	Source Map	Seismic Units Present	Average Predicted Intensity Increment
106. Tmsl	Miocene siltstone with minor sandstone	EBay	III, IV	0.4
107. Tms	Miocene unnamed sandstone, siltstone and shale	NC	II	0.7
108. Tmc	Miocene non-marine clay	EBay	II	0.7
109. Tmsa	Miocene tan fine-grained sandstone, local basal conglomerate	EBay	II, IV	0.5
110. Ttv	Miocene dacite and rhyolite dacite tuff breccia	SWSC	III, IV, VII	0.2
111. Tus	Miocene unnamed sandstone	SM; NWSC	I	1.0
112. Tmsh; Tmc; Tma; Tm	Miocene silty-siliceous gray shale (including the Monterey Shale & upper Claremont Shale)	EBay; SWSC; SM; NWSC	II, III	0.6
113. Tt	Miocene Tice Shale	Oak	II, III, V	0.5
114. Tmsc; Tmi	Miocene brittle cherty-siliceous shale (including the Claremont Shale and lower Claremont Shale)	EBay; Oak	II, III, IV	0.5
115. Tms; Tmso	Miocene basal sandstone (including the Sobrante Sandstone & Temblor Sandstone)	EBay; SWSC; Oak	IV, V, VI	0.2
116. Ts; Tmsr	Miocene sandstone (including the San Ramon Formation)	NE; EBay	III, IV	0.4
117. Tpm	Miocene Page Mill Basalt	SM; NWSC	III, IV, V, VI, VII	0.2
118. Tmsu	Miocene unnamed graywacke sandstone	EBay	I, II	0.8
Tertiary Units (Miocene/Oligocene)				
119. Tuv	Miocene/Oligocene unnamed volcanic rocks	SM	III, IV, V, VI, VII	0.2
120. Tls	Miocene/Oligocene Lambert Shale and San Lorenzo Fm.	SM; NWSC	I	1.0
121. Tla	Miocene/Oligocene Lambert Shale	SWSC; SM; NWSC	II, III	0.6
122. Tmb	Miocene/Oligocene Mindego Basalt and related volcanic rocks	SM; NWSC	III, IV, V, VI, VII	0.2
123. Tlo	Miocene/Oligocene Lompico Sandstone	SWSC; SM	V	0.2
124. Tvq	Miocene/Oligocene Vaqueros Sandstone	SWSC; SM; NWSC	V	0.2
125. Tb	Miocene/Oligocene basalt and diabase flow and sills	SWSC; SE	VII	-0.2
126. Tui	Miocene/Oligocene unnamed marine shale--siliceous and clay shale	EBay	II, III	0.6
127. Tuc	Miocene/Oligocene unnamed marine shale--clay shale and minor sandstone	EBay	II, III	0.6
Tertiary Units (Oligocene)				
128. Tkt	Oligocene Kirger Formation--tuff	EBay	II	0.7
129. Tks	Oligocene Kirger Formation--tuffaceous sandstone	EBay	I, II	0.8
Tertiary Units (Oligocene/Eocene)				
130. Tsl	Oligocene/Eocene San Lorenzo Formation	SWSC; SM; NWSC	I	1.0
131. Tsr	Oligocene/Eocene Rices Mudstone Member of the San Lorenzo Formation	SWSC; SM; NWSC	I	1.0
132. Tst	Oligocene/Eocene Twobar Shale Member of the San Lorenzo Formation	SWSC; SM	I	1.0
Tertiary Units (Eocene)				
133. Tb	Eocene Butano Sandstone south of La Honda	SWSC; SM; NWSC	II, III, IV, V, VI	0.3
134. Tb	Eocene Butano Sandstone north of La Honda	SM	II, III, IV, V, VI	0.3
135. Tbs	Eocene shale in the Butano Sandstone	SWSC; SM	I	1.0
136. Tb?	Eocene Butano Sandstone--questionable	SM; NWSC	I	1.0
137. Tt	Eocene Tolman Formation--sandstone and siltstone	EBay	IV, V	0.2
138. Tk	Eocene Kreyenhagen Formation	NE; EBay	I, II	0.8
139. Tksh	Eocene Kreyenhagen Formation--semi-siliceous shale	NE; EBay	II	0.7
140. Tkm; Tem, Tmk	Eocene Markley Sandstone of Kreyenhagen Formation	NE; CE; EBay	I, II	0.8
141. Tems; Tmu	Eocene Markley Sandstone of Kreyenhagen Formation--Upper sandstone unit	NE; EBay	I, II	0.8
142. Tml	Eocene Markley Sandstone of Kreyenhagen Formation--lower sandstone unit	CE	I, II	0.8
143. Tkn; Tnv	Eocene Nortonville Shale of Kreyenhagen Formation	NE; CE; EBay	II	0.7
144. Tenu	Eocene Nortonville Shale of Kreyenhagen Formation--upper shale unit	NE	II	0.7
145. Tenm	Eocene Nortonville Shale of Kreyenhagen Formation--middle sandstone unit	NE	II, V	0.4
146. Ten?	Eocene Nortonville Shale of Kreyenhagen Formation--lower shale unit	NE	II	0.7
147. Tds; Ted; Td	Eocene Domengine Sandstone--tan, arkosic	NC; NE; CE; EBay	I, V	0.6
148. Tec	Eocene Capay Formation--brown and gray shale and sandy mudstone	NE	II, III	0.6
149. Tmg	Eocene Meganos Formation--undivided; some parts queried	EBay	I, II	0.8
150. Tmge; Tme	Eocene Meganos Formation--Division E, greenish gray marine silty mudstone	CE; EBay	II	0.7
151. Tmgd; Tmd	Eocene Meganos Formation--Division D, light gray marine sandstone	CE; EBay	V, I, II	0.9

Map Symbol (s)	Geologic Unit	Source Map	Seismic Units Present	Average Predicted Intensity Increment
152. Tmgc; Tmc	Eocene Meganos Formation--Division C, bluish gray marine shale; many sandstone interbeds locally mapped	CE; EBay	I, II	0.8
153. Tmgs; Tmcs	Eocene Meganos Formation--sandstone interbeds locally mapped within Division C	EBay	I, II	0.8
154. Tmga; Tma	Eocene Meganos Formation--Divisions A and B, basal grayish brown marine sandstone	CE; EBay	I, II	0.8
155. Tmgs	Eocene sandstone within Meganos Formation	EBay	I, II	0.8
156. Tts	Eocene Tesla Formation	EBay	II	0.7
157. Tss	Eocene Tesla Formation--medium-grained sandstone, minor clay shale	EBay	II	0.7
158. Tss	Eocene unnamed sandstone and shale	Oak	II, VI	0.4
159. Tss	Eocene unnamed sandstone and shale in southwest Santa Clara County	EBay; SWSC	II, III, IV, VI	0.4
160. Tss; Ts	Eocene unnamed sandstone in SW Santa Clara County	SWSC	II	0.7
161. Tls	Eocene unnamed limestone in SW Santa Clara County	SWSC	III, IV, VII	0.2
Tertiary Units (Eocene/Paleocene)				
162. Tsh; Tssh	Eocene/Paleocene marine shale and micaceous shale in southwest Santa Clara County	EBay; SWSC	II	0.7
163. Tg	Eocene/Paleocene strata of German Rancho	NW	IV, V, VI	0.2
Tertiary Units (Paleocene)				
164. Tss	Paleocene unnamed sandstone and shale	SM	III, IV, VI	0.3
165. Tpu	Paleocene unnamed shale with sandstone	NE	II	0.7
166. Tpus	Paleocene unnamed shale--upper sandstone member	NE	II	0.7
167. Tmz	Paleocene Martinez Formation	NE; EBay	II	0.7
168. Tpmu	Paleocene Martinez Formation--upper member; silty mudstone and shale	NE	II	0.7
169. Tpm?	Paleocene Martinez Formation--lower member; sandstone	NE; EBay	II	0.7
170. Tp	Paleocene Pinehurst Shale	Oak	II, III	0.6
171. Tv	Paleocene Vacaville Shale of Merriam and Turner	NC	II	0.7
172. Tl	Paleocene Laird Sandstone	CMm	IV, V, VI	0.2
173. Tpr	Paleocene conglomerate at Point Reyes	CMm	V, VI	0.1
Tertiary (Paleocene)/Cretaceous Units				
174. TKpr	Lower Tertiary/Upper Cretaceous Pinehurst Shale and Redwood Canyon Formation	Oak	II, III, IV, V	0.4
175. TKu	Lower Tertiary/Upper Cretaceous undifferentiated sandstone, mudstone and conglomerate of Stewards Point quadrangle	NW	II, IV, V	0.4
176. TKpr	Lower Tertiary/Upper Cretaceous unnamed shale; marine clay shale and minor thin sandstone of Santa Clara County	EBay; SWSC	II, III	0.6
177. TKss	Lower Tertiary/Upper Cretaceous unnamed marine arkosic sandstone of Santa Clara County	SWSC	V, II	0.9
178. KTsh; KTs	Lower Tertiary/Upper Cretaceous unnamed micaceous clay shale, siltstone	EBay; SE	II, III	0.6
179. KTs	Lower Tertiary/Upper Cretaceous sandstone within unnamed shale, siltstone	EBay	III, IV, V	0.3
180. KTsh with circles	Lower Tertiary/Upper Cretaceous conglomerate within unnamed shale, siltstone	EBay	V	0.2
181. KTsh with dashes	Lower Tertiary/Upper Cretaceous limestone within unnamed shale, siltstone	EBay	VI	0.0
Cretaceous Units				
182. Ku	Upper Cretaceous rocks, undivided Great Valley Sequence	Oak	II, III, IV, V	0.4
183. Kss	Upper Cretaceous marine sandstone and shale in southwest Santa Clara County	SWSC	II, III, VI	0.4
184. Ksh	Upper Cretaceous marine micaceous shale in southwest Santa Clara County	SWSC	IV, V, VI	0.2
185. Kcg	Upper Cretaceous marine pebble conglomerate in southwest Santa Clara County	SWSC	V, VI	0.1
186. Kcg	Cretaceous conglomerate and sandstone, unnamed	EBay	V, VI	0.1
187. Ksh	Cretaceous dark shale, unnamed	EBay	II, III	0.6
188. Ka	Cretaceous strata of Anchor Bay	NW	II, IV, VI	0.3
189. Ks	Cretaceous strata of Stewards Point	NW	II, IV, VI	0.3
190. Ksb	Cretaceous spilite (sodic basalt) near Black Point on Stewards Point quadrangle	NW	VII	-0.2
191. Kpp	Cretaceous Pigeon Point Formation	SM	V, VI	0.1
192. Kgr	Cretaceous granitic rocks of Montara Mountain	SM	VII	-0.2
193. Kgr	Cretaceous granitic rocks at Bodega Head	NW	VII	-0.2
194. gr, Kgr	Cretaceous granitic rocks in Marin County	CMm	VII	-0.2

Map Symbol (s)	Geologic Unit	Source Map	Seismic Units Present	Average Predicted Intensity Increment
195. Ksh	Cretaceous unnamed shale	SM	I	1.0
196. KJgv	Cretaceous/Jurassic Great Valley Sequence undifferentiated	NW	II, III, IV, V	0.4
197. Km	Cretaceous Great Valley Seq. Moreno Shale--clay shale	CE; EBay	II, III	0.6
198. Kms	Cretaceous Great Valley Seq. Moreno Shale--sandstone	CE; EBay	II, VI	0.4
199. Kmi	Cretaceous Great Valley Sequence Moreno Shale--semi-siliceous shale	EBay	II, III	0.6
200. Kps (also Kj)	Cretaceous Great Valley Sequence Panoche Formation buff arkosic sandstone, minor shale	CE; EBay	III, IV, V, VI	0.2
201. Kpc	Cretaceous Great Valley Sequence Panoche Formation--cobble conglomerate and sandstone	EBay	V, VI	0.1
202. Kp (also Kmu)	Cretaceous Great Valley Sequence Panoche Formation--micaceous shale, minor thin sandstone beds	CE; EBay	II, III	0.6
203. Kpl	Cretaceous Great Valley Sequence Panoche Formation--marine clay shale, minor sandstone	EBay	IV, V	0.2
204. Kdv	Cretaceous Great Valley Sequence Deer Valley Formation--arkosic sandstone	CE; EBay	IV, V	0.2
205. Ks	Cretaceous Great Valley Seq. unnamed marine clay shale	EBay	IV, V	0.2
206. Ksh	Cretaceous Great Valley Sequence marine micaceous shale, undivided	EBay	II, III, IV	0.5
207. Kcg; cg	Cretaceous Great Valley Sequence conglomerate younger than marine shale	EBay	V	0.2
208. Kshu	Cretaceous Great Valley Seq. Berryessa Fm., undivided	EBay	III, IV, V, VI	0.2
209. Kshb	Cretaceous Great Valley Sequence shale within the Berryessa Formation	EBay; SE	III, IV	0.4
210. Ksg	Cretaceous Great Valley Sequence sandstone and conglomerate within the Berryessa Formation	EBay	VI	0.0
211. Kss	Cretaceous Great Valley Sequence sandstone within the Berryessa Formation	EBay	V, VI	0.1
212. Kr	Cretaceous Great Valley Sequence Redwood Canyon Fm.	Oak	IV, V	0.2
213. Ks	Cretaceous Great Valley Sequence Shephard Creek Fm.	Oak	II, III	0.6
214. Kcg; Kcgo	Cretaceous Great Valley Sequence Oakland Conglomerate	EBay; SE; Oak	IV, V	0.2
215. Kjm	Cretaceous Great Valley Sequence Joaquin Miller Fm.	Oak	III, IV, V	0.3
216. Ku	Cretaceous Great Valley Sequence unnamed formation sandstone and shale, undivided	NE	II, III, VI	0.4
217. Kuu	Cretaceous Great Valley Sequence unnamed formation--upper sandstone member	NE	II, VI	0.4
218. Kul	Cretaceous Great Valley Sequence unnamed formation--lower shale member	NE	II, III	0.6
219. Kfo	Cretaceous Great Valley Sequence Forbes Fm. of Kirby	NE	IV	0.3
220. Kg	Cretaceous Great Valley Sequence Guida Fm. of Kirby	NE	III, V, VI	0.2
221. Kf	Cretaceous Great Valley Sequence Funks Fm. of Kirby	NE	V, VI	0.1
222. Ks	Cretaceous Great Valley Sequence Sites Fm. of Kirby	NE	III, V, VI	0.2
223. Ky	Cretaceous Great Valley Sequence Yolo Fm. of Kirby	NE	III, V, VI	0.2
224. Kv	Cretaceous Great Valley Sequence Venado Fm. of Kirby	NC; NE	VI	0.0
225. Kgvs	Cretaceous Great Valley Sequence unnamed sandstone, mudstone, shale and conglomerate	NC; NE	IV, V, VI	0.2
Cretaceous/Jurassic Units				
226. KJgvm	Cretaceous/Jurassic Great Valley Sequence unnamed fm.--mudstone, shale, siltstone, sandstone and conglomerate	NC; NE	II, III	0.6
227. KJgrs	Cretaceous/Jurassic Great Valley Sequence siltstone with minor sandstone	NW	II, III	0.6
228. KJv	Cretaceous/Jurassic unnamed volcanic rocks	SM	III, IV, V, VI, VII	0.2
229. KJs	Cretaceous/Jurassic unnamed sandstone	SM	V, VI	0.1
230. KJs	Cretaceous/Jurassic shale in SW Santa Clara County	SWSC	IV	0.3
231. KJa	Cretaceous/Jurassic argillite in SW Santa Clara County	SWSC	IV	0.3
232. Kshl; JKk	Cretaceous/Jurassic Great Valley Sequence Knoxville Formation shale with sandstone	EBay; Oak; WAla	II, III, IV	0.5
233. JKc	Cretaceous/Jurassic Great Valley Sequence Knoxville Formation conglomerate and sandstone	EBay	III, IV	0.4
234. Jk	Cretaceous/Jurassic Great Valley Sequence Knoxville Formation siltstone	NC	IV	0.3
235. Jk	Cretaceous/Jurassic Great Valley Sequence Knoxville Formation mudstone and shale	NE	IV	0.3
236. KJgvc	Cretaceous/Jurassic Great Valley Sequence Novato Conglomerate and unnamed conglomerate	NW; CMm	IV, V	0.2
237. KJgv	Cretaceous/Jurassic Great Valley Sequence sandstone with claystone	CMm	III, IV, V, VI	0.2

Map Symbol (s)	Geologic Unit	Source Map	Seismic Units Present	Average Predicted Intensity Increment
238. KJgvs	Cretaceous/Jurassic Great Valley Sequence sandstone, shale and conglomerate	CMrn	III, IV, V	0.3
239. bd	Cretaceous/Jurassic basalt and diabase	SWSC	VII	-0.2
240. vb	Cretaceous/Jurassic volcanic rocks	EBay	VII	-0.2
241. vb	Cretaceous/Jurassic basalt in SW Santa Clara County	SWSC	VII	-0.2
242. vd	Cretaceous/Jurassic diorite in SW Santa Clara County	SWSC	VII	-0.2
243. KJsp; Jsp	Cretaceous/Jurassic Great Valley Sequence sedimentary serpentine	NC; NE	II, III, IV	0.5
244. Jv	Jurassic basaltic pillow lava and breccia at the base of the Great Valley Sequence	NW; NC; NE	III, VI, VII	0.1
245. Jd	Jurassic diabase, gabbro, etc. at the base of the Great Valley Sequence	NW	VII	-0.2
246. Ju	Jurassic ultramafic rock at the base of the Great Valley Seq.	NW	III, VII	0.2
Cretaceous/Jurassic Franciscan Assemblage and Small Masses				
247. KJf	Cretaceous/Jurassic Franciscan Assemblage, undifferentiated	EBay; SM; NWSC; WAla	II, III, IV, V, VI, VII	0.2
248. KJfss; fs; gwy; KJfs; KJs	Cretaceous/Jurassic Franciscan Assemblage, graywacke sandstone, some local shale	NW; CMrn; EBay; SE; SM; SSF; NSF; Oak; NWSC; WAla	III, VI	0.2
249.KJsh	Cretaceous/Jurassic Franciscan Assemblage, shale with some sandstone	NSF; NWSC; WAla	III	0.5
250. KJfg; fg; gs	Cretaceous/Jurassic Franciscan Assemblage greenstone	NW; NC; NE; CMrn; EBay; SE; SM; SSF; NSF; Oak; NWSC; WAla	VII	-0.2
251. KJfm	Cretaceous/Jurassic Franciscan Assemblage metagraywacke and other metamorphic rocks	NW; NC; NE; CMrn; SE; NSF	VII	-0.2
252. KJfs; fsr; KJu	Cretaceous/Jurassic Franciscan Assemblage melange or sheared rocks	NW; NC; NE; CMrn; EBay; SE; SM; SSF; NSF; NWSC	II, III, IV, V, VI	0.3
253. fm; KJfm	Cretaceous/Jurassic Franciscan Assemblage metamorphic rocks	EBay; SM; SSF; Oak	VII	-0.2
254. br	Cretaceous/Jurassic fault (?) breccia	EBay	II, III	0.6
255. r	Cretaceous/Jurassic Franciscan Assemblage hard monolithic fragments	EBay	VII	-0.2
256. ch & gs	Cretaceous/Jurassic chert and greenstone	CMrn	III, VII	0.2
257. mch	Cretaceous/Jurassic metachert	NE	III	0.5
258. ch; fc; KJfc	Cretaceous/Jurassic Franciscan Assemblage chert	NW; NC; NE; CMrn; EBay; SE; SM; SSF; NSF; Oak; NWSC; WAla	III	0.5
259. mgs	Cretaceous/Jurassic greenstone and schistose rocks	NE	II, III, VII	0.3
260. m, pKm	Cretaceous/Jurassic and pre-Cretaceous high-grade metamorphic rocks	NW; NC; NE; CMrn; SE	IV, V, VI, VII	0.1
261. gl	Cretaceous/Jurassic glaucophane schist	EBay	III, IV, V, VI, VII	0.2
262. m	Cretaceous/Jurassic marble and hornfels	SM	IV, V, VI, VII	0.1
263. fl	Cretaceous/Jurassic Franciscan Assemblage limestone	SM; EBay; NWSC; WAla	IV, V, VI, VII	0.1
264. tr	Cretaceous/Jurassic travertine	EBay	IV, V, VI, VII	0.1
265. sc	Cretaceous/Jurassic silicacarbonate rocks	NW; NC; CMrn; EBay	III, IV, V, VI, VII	0.2
266. ////	Cretaceous/Jurassic hydrothermally altered rocks	CMrn	III, IV, V, VI	0.2
267. fcg	Cretaceous/Jurassic Franciscan Assemblage conglomerate	CMrn; SM	III, IV, V, VI	0.2
268. sp	Cretaceous/Jurassic serpentine or serpentinite	NW; NC; NE; CMrn; EBay; SE; SM; SSF; NSF; Oak; NWSC; WAla	II, III, IV, V, VI	0.3
269. spr	Cretaceous/Jurassic serpentine rubble	EBay	II, III, IV, V, VI	0.3
270. db	Cretaceous/Jurassic diabase	EBay	VII	-0.2
271. an	Cretaceous/Jurassic andesite	EBay	VII	-0.2
272. gb	Cretaceous/Jurassic gabbrodiabase	EBay; NSF; Oak	VII	-0.2
273. ##	Cretaceous/Jurassic foliate metabasalt	NW	III, VII	0.2
274. mi	Cretaceous/Jurassic mafic intrusive rocks (gabbro & diorite)	NC	VII	-0.2
275. vk	Cretaceous/Jurassic kertophyre	EBay	VII	-0.2
276. di	Cretaceous/Jurassic diorite and diabase	EBay	VII	-0.2
277. qg	Cretaceous/Jurassic hornblende quartz-gabbro	EBay	VII	-0.2

ABAG ASSOCIATION OF BAY AREA GOVERNMENTS

MetroCenter
Eighth & Oak Streets
Oakland
(510) 464-7900

Mailing Address:
P.O. Box 2050
Oakland, CA 94604-2050

EARTHQUAKE PREPAREDNESS PROGRAM